Pontificia Universidad Católica del Perú

Escuela de Posgrado

Design of the system control for a quantum entanglement optical alignment system

Tesis para obtener el grado académico de Maestra en Ingeniería Mecatrónica que presenta:

Sara Lucía Montaño Gamarra

Asesor PUCP (PUCP): *Prof. Dr.-Ing. Gustavo Pérez Zuñiga*

Co-Asesor de la Universidad no PUCP: *AOR PD Dr.-Ing. habil Tom Ströhla*

Lima, 2025

Informe de Similitud

Yo, **Carlos Gustavo Pérez-Zuñiga**, docente de la Escuela de Posgrado de la Pontificia Universidad Católica del Perú, asesor(a) de la tesis/el trabajo de investigación titulado **Design of the system control for a quantum entanglement optical alignment system**, del autor:

Sara Lucía Montaño Gamarra

dejo constancia de lo siguiente:

- El mencionado documento tiene un índice de puntuación de similitud de 3%. Así lo consigna el reporte de similitud emitido por el software *Turnitin* 17/07/25
- He revisado con detalle dicho reporte y la Tesis o Trabajo de Suficiencia Profesional, y no se advierte indicios de plagio.
- Las citas a otros autores y sus respectivas referencias cumplen con las pautas académicas.

Lugar y fecha: 21/07/25

Apellidos y nombres del asesor / de la asesora: **Pérez-Zuñiga, Carlos Gustavo**	
DNI: 41864666	Firma: 
ORCID: 0000-0001-5946-1395	

Dedico esta tesis a mis padres, quienes me enseñaron el valor del esfuerzo y la perseverancia, gracias por ser mi inspiración y mi mayor fuente de apoyo en este camino; a mi hermano, compañero de profesión y de vida, cuyo conocimiento y respaldo han sido fundamentales para alcanzar esta meta; a mi familia, por su amor constante; y a mis amigos, por su compañía y por recordarme siempre que las grandes metas son más fáciles de alcanzar cuando se comparten.

I deeply thank my colleague and friend, Ph.D Pablo Cárdenas, for his invaluable guidance and teaching throughout this process, as well as for being a constant mentor in my academic and professional development.

I also want to thank MSc. Rana Sebak for her initial contribution to defining the project and the support provided in the laboratory.

I extend my gratitude to the Pontifical Catholic University of Peru and the Technical University of Ilmenau for their support and the opportunity to pursue this double degree program. I am especially grateful for the professors who selected me to continue my studies in Germany. I also acknowledge the Fraunhofer IOF for providing the infrastructure and resources essential for the successful development of this project.

Resumen

Esta tesis tiene como objetivo diseñar un sistema de control para una configuración de alineación óptica cuántica, con el fin de aumentar la probabilidad de recolectar pares de fotones en un sistema de fotones entrelazados.

El diseño incluye la fabricación de componentes impresos en 3D para motorizar los soportes del espejo cinemático y la lógica de control para ocho motores paso a paso, todo ello gestionado por un microcontrolador de 32 bits. El desarrollo abarca los aspectos mecánicos, de control y de software, incluyendo la transmisión de instrucciones de control del motor y el almacenamiento de datos de movimiento para fines de aprendizaje.

Se han probado tanto los componentes mecánicos como los eléctricos y se han recopilado datos, lo que ha revelado errores que se han corregido en iteraciones posteriores del sistema. Si bien se presentan los resultados de la simulación, no se incluyen los resultados finales de la implementación debido a limitaciones de tiempo para experimentos adicionales. Se requieren más pruebas y mejoras para validar completamente el rendimiento del sistema.

Abstract

This thesis aims to design a control system for a quantum optical alignment setup, with the goal of increasing the probability of collecting photon pairs in an entangled photon system.

The design includes the fabrication of 3D-printed components used to motorize the kinematic mirror mounts and the control logic for eight stepper motors, all managed by a 32-bit microcontroller. The development covers the mechanical, control, and software aspects, including the transmission of motor control instructions and the storage of movement data for learning purposes.

Both the mechanical and electrical components have been tested, and data has been collected, revealing errors that have been addressed in subsequent iterations of the system. Although the simulation results are presented, the final implementation results are not included due to time constraints for additional experiments. Further testing and refinement are required to fully validate the system's performance.

Table of Contents

List of Illustrations

List of Tables

Chapter 1

Introduction

1.1 Problem Statement

Quantum entanglement has been the subject of increasing studies because of its vast potential to revolutionize current technologies and not only in the computing and communication fields. Photon experiments are one of the most alluring quantum physical sensations. Due to their notable features, Einstein, Podolsky, and Rosen (EPR) examined in 1935. The authors observe that the predictions for a two-particle state indicate that, despite their arbitrary separation, they constitute a unified entangled system [1]. This phenomenon holds immense promise the advancement of quantum information, imaging, and communication technologies [2], [3]. However, manual alignment of light beams in these experiments is prone to inefficiencies due to environmental changes, requiring frequent realignment and increasing experimental time.

The alignment of light beams is essential in the optical field and crucial in experiments with entangled photons that need to simultaneously detect as many photons as possible [4], allowing for further studies, such as molecular absorption analysis [5]. Despite various studies proposing improvements to manual mounts [6, 7, 8], these systems still exhibit angular movement when subjected to temperature variations. Environmental fluctuations also require frequent realignments, leading to time-consuming processes and reduced experimental efficiency.

To address these challenges, automated optical mirror mounts present a promising alternative. These systems can significantly reduce alignment time, enhance precision, and improve the overall process. While commercial solutions exist that utilize technologies like DC servo motors, stepper motors, or piezoelectric actuators, these models are often expensive, they often come with a higher cost compared to more accessible alternatives like stepper motors with microstepping, which can still

offer sufficient precision for many applications.

Furthermore, the evolution of 3D printing and open-source hardware and software has made it possible to create cost-effective and modifiable solutions for quantum optics research [9]. These advances provide opportunities to innovate in the production of mechanical equipment and the automation of optical alignment systems, which are critical for the advancement research in this field.

The project was designed using open source software and custom-built components, including 3D-printed components to ensure flexibility and avoid reliance on a specific manufacturer. This approach allows for full control over the system's design and adaptability to specific requirements.

1.2 Motivation

One of the challenges in quantum optics research is the precise alignment of light beams. Manual alignment can take several hours or even days. Automating this process can significantly improve precision and reduce alignment time.

The fact that automated alignment processes often use standardized and high-cost components. The motivation behind this work is to develop a complete system is the main goal, starting from the design of 3D-printed, the creation of a custom PCB and the control logic focus in the data acquisition from photon detection and no need to configure specific parameters related to mirror mount angles or positions.

The 3D-printed parts should be able to adapt to the mirror mount position and its knobs position. Additionally, the PCB will be able to receive information via serial communication to determine which motor to control, enabling precise position adjustments.

1.3 Goals of the project

This thesis aims to design a complete system that includes the 3D printed structure and electronic circuit design, targeting the alignment of signal and idler photons, maximizing coincidence counting between the signal and idler.

The proposed system integrates:

- Design the mechanical support structure for the motors adaptable to optical kinematic mounts, ensuring cost-effectiveness.
- Develop and optimize the electronic design necessary for the implementation of a control algorithm that allows the reading and analysis of data every 100ms.
- A data storage mechanism to record motor movements and positions, enabling efficient alignment adjustments.
- A position controller for eight programmable stepper motors with a resolution of less than 1 arcsecond.

This solution aims to enhance the precision and efficiency of optical alignment in quantum optics experiments, contributing to advancements in the field.

Chapter 2

Fundamentals and design strategies

Automation of optical mounts has gained interest in recent years, with the development of motorized systems adaptable to various optical applications. The use of 3D printing and open-source hardware/software has facilitated the customization of these systems, allowing for flexible and low-cost designs. Some approaches have incorporated microcontrollers such as Arduino and embedded computers such as Raspberry Pi, along with optimization algorithms.

2.1 Quantum Entanglement Basics

Photon-based experiments leverage the phenomenon of quantum entanglement, which allows correlated behaviors between photons even when separated by large distances. While this thesis does not delve into the theoretical details and the research has specific applications, the adaptable design could be used for other experiments in the field of quantum optics.
Some of the most important examples of the use of quantum entanglement highlighting its relationship to alignment and applications:

- **Quantum Key Distribution (QKD):**

  In 1991, Artur Ekert [10] proposed the first application of quantum information theory based on entanglement, known as quantum key distribution (QKD). Ekert introduced the use of Einstein-Podolsky-Rosen (EPR) entangled pairs to generate private cryptographic keys.

  In quantum cryptography based on the BB84 or Ekert protocol, if ”c” tries to listen to the quantum bits transmitted between ”A” and ”B”, the nature of quantum mechanics generates detectable disturbances in the communication, alerting ”A” and ”B” to their presence.

  The first experimental implementations of the Ekert protocol used entangled photons obtained

by spontaneous parametric conversion [11] and energy- and time-entangled photons [12]

- **Quantum dense coding:**

  The concept of dense coding, developed by Bennett and Wiesner in 1992 [13], allows us to overcome the limit imposed by the Holevo bound [14], which states that a qubit can transmit at most one bit of classical information.

  In this protocol, Alice can send two classical bits using only one qubit, provided that she has previously shared a pair of entangled qubits (EPR state) with Bob.

- **Quantum teleportation:**

  Bennett et al. [15] proposed that an unknown qubit can be ”teleported” from Alice to Bob using entanglement and classical communication. This technique is fundamental in quantum networks for the secure and faithful transfer of quantum information.

For a review of the basic aspects of entanglement, including its characterization, detection, distillation, and quantification, see Horodecki et al. (2009) [16]

2.2 Light Beam Alignment in Optics

Proper alignment is crucial to ensure that entangled photons maintain their coherence and the properties needed for applications in quantum communication and computing.
There are a variety of mechanisms for the control and alignment of optical beams, basically the following:

- **Manual Angular Alignment:**

  Manual stages for angular alignment are discussed, including systems such as three-contact gimbals, flexible hinges, and rotating wedges. Displacement curves and deflection nomograms are presented with analytical formulas for reference.

- **Manual and Motorized Translation Stages:**

  Protopopv [17] provides concentrated information on manual and motorized translation stages that can be found in the laboratory. Practical recommendations are offered to improve the performance of these stages, including detailed explanations of stepper motors, connection diagrams, controllers, micro-stepping modes, electromagnetic noise, and vibrations, illustrated with experimental oscillograms.

Beam alignment involves to precisely adjust the angle's mirror. Various analyses [18] discuss advances in the use of orbital angular momentum and entangled vector states, combining spatial modes with polarization. These states require meticulous control of light patterns, where precise alignment of mirrors is essential to generate and manipulate structured light states. Improper alignment can compromise the quality of entanglement and the efficiency of quantum systems. Moreover, these systems are highly sensitive to environmental changes and susceptible to misalignments caused by factors such as temperature variations [19].

2.3 Automated Optical Mounts

Various automation options that use motors have been presented, such as a mirror-mounted control system that is flexible, easy to build, inexpensive, and computer controlled. This section details some of the most relevant systems.

One system was developed in 2015 [20] for undergraduate research laboratories and uses geared motors, commonly used in hobby robotics, which are controlled by an Arduino microcontroller in combination with an H-bridge to precisely position the mirror mount actuators. In addition, a graphical user interface based on the Python programming language is provided. The total cost of the system is a fraction of the price of commercially available systems.

On the other hand, an automated laser beam alignment system based on a Raspberry Pi and NEMA 17 stepper motors connected to optical mounts via metal mechanical couplings has been presented. A Raspberry Pi 4 Model B controls the motors and an ADC converter converts the signal from a photodiode into digital data. L298N motor drivers manage the power and direction of the motors. In addition, the M-LOOP machine learning algorithm is used to optimize the coupling of light into the fiber. It works by identifying the best fit of the mirrors through iterative testing. The optimization process takes approximately 20 minutes. As an advantage, these motors provide higher torque than usual; however, they have disadvantages, their larger dimensions, and excessive weight. In this case, the step motor supports are metallic in an L-form. [21]

Other researchers use near-field and far-field cameras to monitor the beam position. Additionally, they use a Shack-Hartmann sensor to correct defocus. The mirrors are adjusted with stepper motors, and the process is repeated until alignment is achieved. Furthermore, they developed their own software.[22]

2.4 Open-Source Hardware and 3D Printing in Research

Researchers has explored the use of 3D printing technology for manufacturing multiple mechanical components in optical systems. Traditional optical mounts, which are typically made of metal or other rigid materials, can now be fabricated using open-source, 3D-printable designs, significantly reducing costs and enabling customization.

A notable example is the development of parametric optical components, which allow researchers to quickly adapt their designs to specific experimental requirements. These components include mirror mounts, lens holders, fiber optic holders, and filter brackets, all of which can be printed using affordable materials like PLA or ABS. By integrating 3D printing with open-source electronics (such as Arduino-based controllers), researchers can create fully automated optical systems that are highly flexible and cost-effective compared to commercially available solutions[23]. Another project focused on developing an optical cage system for safety purposes, ensuring that radiation does not harm the eyes. Furthermore, the design can also be employed for blackout and noise reduction applications [24].

There are developments where 3D printing in the field of optics has progressed beyond the manufacture of mechanical components, also encompassing the production of optical fibers and integrated optical elements. Methods have been developed to use 3D printing in the creation of preforms that are then converted into silica glass optical fibers. This approach not only simplifies the production of these fibers, but also makes possible designs and applications that were not feasible before. As well as achieving the printing of silica glass micro-optics directly on the tips of optical fibers. This advance could allow for faster internet connections and improvements in connectivity, as well as innovations in more compact sensors and images [25].

Additionally, advanced techniques such as SLA, SLS, DLW and DIW have been used to fabricate optical components with resolutions down to 150 nm. Functional optical components have also been produced using polymeric materials and hybrid composites that can replace certain glass elements in specific applications [26].

2.5 Design Strategies

Recently, research has focused on comparing three different approaches for the optical alignment of a two-mirror system, each with two axes. The study highlights the use of artificial neural networks

(ANNs), which are commonly applied to nonlinear problems. Additionally, it compares this approach with a practice-led method, which mimics human alignment strategies, and a design-led method, which relies on advanced mathematical models. The findings reveal that each method presents trade-offs in terms of computational cost, data requirements, and efficiency. While ANNs require extensive training data, the practice-led approach leverages expert knowledge, and the design-led approach depends on precise mathematical modeling. The study contributes valuable insights into the automation of optical alignment, with potential applications in telescopes, interferometers, and laser-based systems.[27]

Another research proposed a design using 3D- printed components, an Arduino Uno board, and step motors 28BYJ-48, allowing control of five kinematic mounts. The implementation involved using MATLAB and a Thorlabs PM100-A detector. The auto-alignment procedure entailed scanning the X-Y plane in two steps and detecting the maximum power, first in the X direction and then in the Y direction [28].

Chapter 3

Proposal design

The present chapter shows the system control design for a quantum optical alignment system. For the proposed design, the VDI 2201 design method will be used in general, which is recommended for the present case.

3.1 System Overview

This system is designed to optimize the alignment of entangled photons in a quantum optics experiment. It consists of four optical mirrors positioned at the final stage of the quantum entanglement setup. The proposed alignment system adjusts mirrors 1 to 4 to maximize the detection of both signal and idler photons, using real-time feedback from the time tagger.
The following figure 3.1 illustrates the optical alignment setup, highlighting in the orange box the key components involved in the alignment process, such as the mirrors and their connections to the time tagger channels.

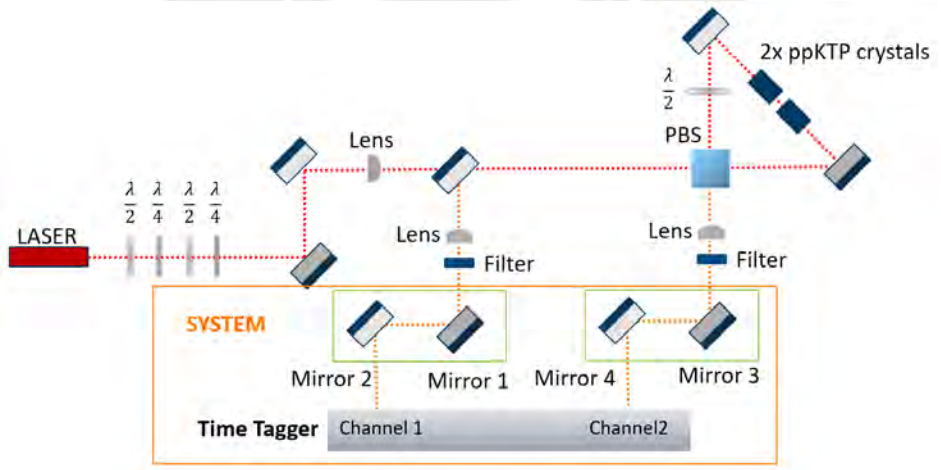

Figure 3.1: System Overview [Redrawn and adapted by Sara Montano from Rana Sebak, based on Phys. Rev. Lett. 121, 200502.]

3.2 Conceptual Design of the Prototype System

The image 3.2 shows in the orange box, two types of kinematic mirrors of the optical system used in the experiment. These mirrors are intended to be automated in order to optimize their alignment by controlling yaw and pitch movements through attached motors. It is observed that the movements in the yaw and pitch of mirrors 1 and 2 directly affect the amount of photons detected in channel 1 of the time tagger, just as mirrors 3 and 4 affect the amount of photons in channel 2. Since coincidences refer to the simultaneous detection of entangled photon pairs in both channels, any adjustment to the mirrors impacts the coincidence rate.

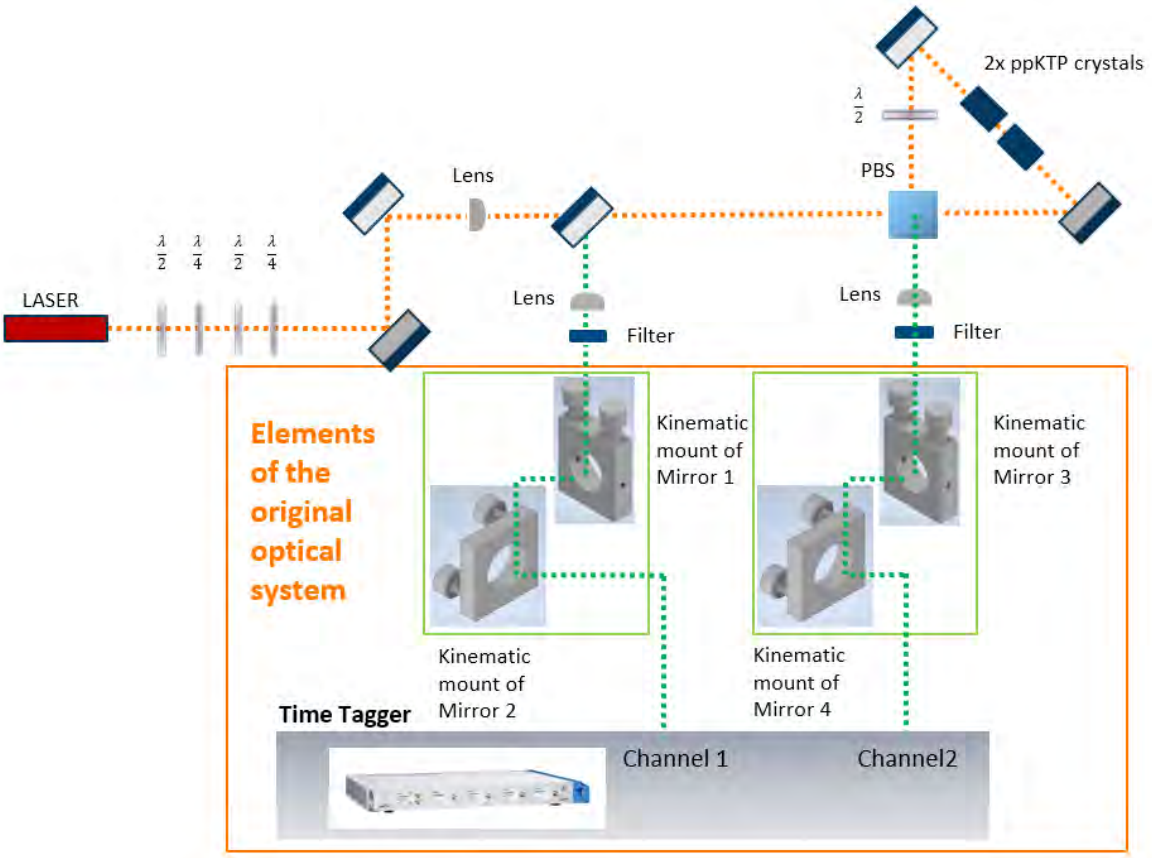

Figure 3.2: Optical system used in the experiment

Automating the kinematic mirror mounts is essential to achieve maximum photon counts and coincidences. This requires defining a set of specifications for the alignment of the four mirrors, considering the mechanical structure needed to support and attach the motors to the kinematic mounts, the associated electrical connections, and the control systems that ensure efficient operation.

Figure 3.3 presents the conceptual design of the automation system. In this image, the motors are highlighted in black, showing their position relative to the kinematic mounts, which are shown in

grey. The figure also illustrates the supporting mechanical structure in beige, along with the electrical connections and control interfaces required for proper functionality.

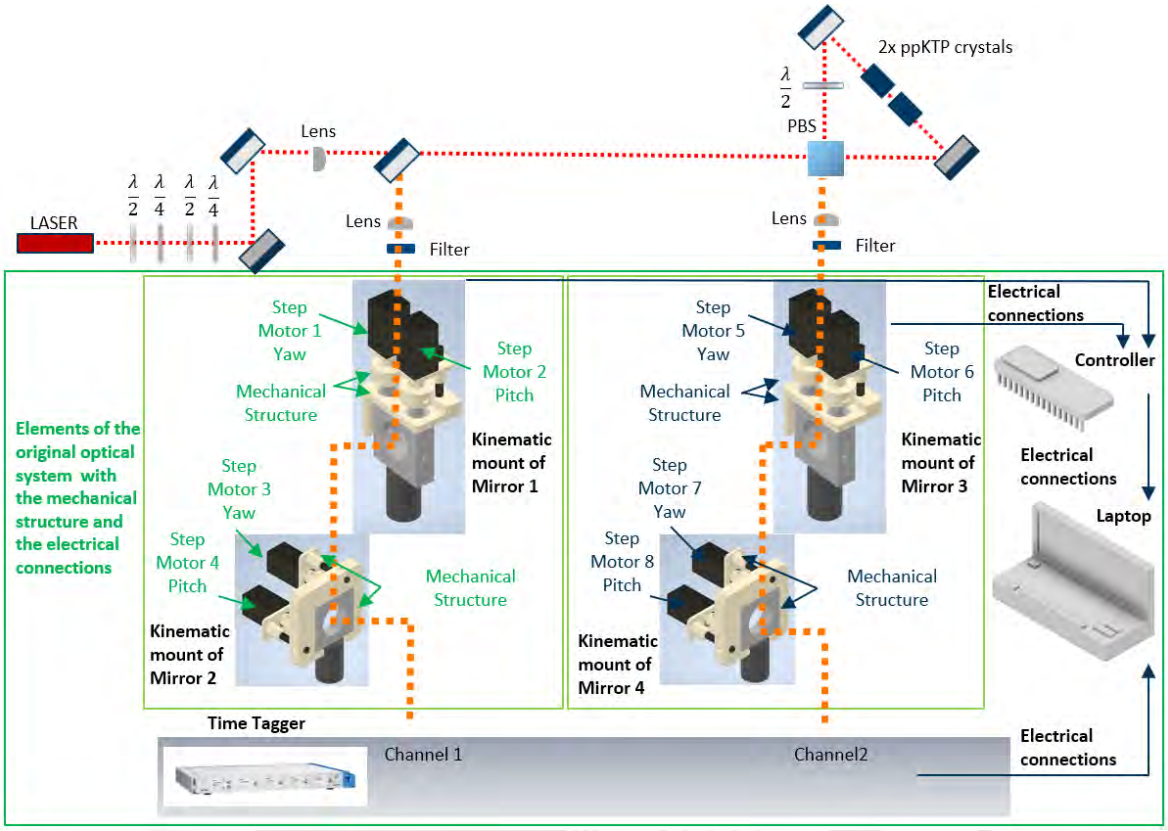

Figure 3.3: Conceptual design of the Optical system used in the experiment

The conceptual design process includes identifying the requirements, structuring the system functions, and developing optimal solution alternatives in the domains.

3.2.1 Requirements List

The design process begins with a comprehensive list of demands and constraints that the system must fulfill. The priority requirements are classified as demands, while additional features are considered desires. Tables 3.1, 3.2, and 3.3 present the list of demands and desires for the design of the quantum optical alignment system.

List of demands			Page 1 of 3
PROJECT:		Design of the system Control for a quantum optical alignment system	Date: 31/03/2023
CLIENT:		PUCP - TU-ILMENAU - FRAUNHOFER	Elaborated: Sara Montano
Date:	Demand or Desire	DESCRIPTION	Responsible: Sara Montano
01/05/2022	Demand or Desire	**PRINCIPAL FUNCTION:** The system must be able to adjust the knobs of the kinematic optical mirror mounts to maximize the coincidence counts between signal and idler photons, as well as the total photon counts. It is important to note that the maximum number of coincidences cannot be defined as a fixed value, since it depends on various experimental conditions such as temperature fluctuations, optical alignment of other components, and the laser intensity. Therefore, the system is designed to dynamically optimize photon detection under the given experimental configuration.	S.L.M.G.
01/06/2022	Demand	**GEOMETRY:** PCB dimensions less than 15cm x 15cm. The connections should be configurable according to the market. The connectors on the PCB must be compatible with the motor wiring. The designed structure should be adaptable. The designed structure must be compatible with M2 and M4 screws. The structure must have couplers to secure the motor base using M2 screws and to connect the motor shaft with the kinematic mount knob, ensuring proper rotational alignment. The structure should integrates a smooth pin that ensures the alignment between the motor and the kinematic mount knob. The structure must be secured to the sides of the kinematic optical mount. The structure must not have a base to avoid lifting the kinematic optical mount. The system must be manufactured in modules, for easy assembly and installation in different places.	S.L.M.G.
01/07/2022	Demand	**ENERGY:** It can be connected to the single-phase electrical network. It will convert AC power to DC. The power supply to the motors will be via cables The energy for the different electronic components is regulated.	S.L.M.G.
01/08/2022	Demand	**SIGNAL (INFORMATION):** The system receives as input signal the photon count of respectively signal and idler of the entangled photon pair. These photon counts are processed by a control algorithm. Based on the analysis, the system generates output signals that are sent to the motor drivers that are connected to the knobs of the kinematic optical mount. As the motors move, the photon counts should be updated to form a closed feedback loop. The updated data is re-evaluated to decide the movement of the motors. The interface should display the number of detected photon counts and the corresponding motor movements.	S.L.M.G.

Tabla 3.1: List of demands part 1

List of demands			Page 2 of 3
PROJECT:		Design of the system Control for a quantum optical alignment system	Date: 31/03/2023
CLIENT:		PUCP - TU-ILMENAU - FRAUNHOFER	Elaborated: Sara Montano
Date:	Demand or Desire	DESCRIPTION	Responsible: Sara Montano
01/08/2022	Demand	**CONTROL REQUIREMENT:** A position control will be carried out for 8 stepper motors. An individual alignment is performed for each motor based on the values from the detection channel. The alignment process includes identifying optimal reference positions, which serve as alignment targets. Maximizing photon counts in both channels increases the likelihood of detecting entangled pairs within a narrow window previously programmed by the user, thereby maximizing the coincidence rate. This process can be understood as an optimization problem, where the objective is to find the motor positions that yield the highest coincidence rate. The individual alignment process should stop within one minute.	S.L.M.G.
01/09/2022	Demand	**ELECTRONICS:** The design of the electronic boards will be carried out. The PCB design must follow the recommendations of the component datasheets and the layout rules. It will transform from 220vAC to 12vDC and 3.3vDC.	S.L.M.G.
01/03/2023	Demand	**SOFTWARE:** Software will be used to design the circuit and the electronic board. Software will be used to design the mechanical drawings of the coupling structure between the optical mirror mount and the motor. **SOFTWARE REQUIREMENTS:** The programming must be compatible with Python, because the time tagger uses Python-based libraries to acquire the data.	S.L.M.G.
01/03/2023	Demand	**COMMUNICATIONS:** Serial communication will be used to send information. The connection of the drivers with their respective motors will be through cables.	S.L.M.G.
01/03/2023	Demand	**SECURITY: Software Safety Limitation:** The system must include programmed motion limits to avoid forcing the motor against the mechanical stops of the kinematic mounts. In cases where the mirror knob is already at its extreme position (e.g., fully rotated clockwise or counterclockwise), continued motor actuation may result in mechanical stress or damage to the mirror mount or motor. The control algorithm must obtain the position of the motors to analyze and restrict the movement. If it is detected that the mirror is close to its rotation limit, the software must prevent further movements in that direction (as this may generate mechanical stress or damage to the mirror support or the motor). The mechanical structure should minimize mechanical risks due to the low torque and low-voltage nature of the motors. It is recommended that all power supply lines include short circuit and overload protection. A custom printed circuit board (PCB) must be used to properly distribute and limit current flow. The system should stopped by programming when the maximum values are detected or a failure occurs.	S.L.M.G.

Tabla 3.2: List of demands part 2

de	**List of demands**	Page 3 of 3	
PROJECT:		Design of the system Control for a quantum optical alignment system	Date: 31/03/2023
CLIENT:		PUCP - TU-ILMENAU - FRAUNHOFER	Elaborated: Sara Montano
Date:	Demand or Desire	DESCRIPTION	Responsible: Sara Montano
01/03/2023	Demand	**ERGONOMICS:** The design should allow components to be assembled easily, avoiding hard-to-reach screws or parts that require specialized tools. Connectors located in positions that facilitate the quick connection and disconnection of electronic components. Intuitive interface allows for easy parameter adjustments.	S.L.M.G.
01/09/2022	Demand	**FABRICATION:** The prototype PCB version allows the acquisition of modules on the market. The final version needs the specific electronic components list for manufacturing. The parts that must be manufactured with 3D printing will be specified.	S.L.M.G.
01/10/2022	Demand	**MOTOR:** The motor must be bipolar. The motor must be small with a maximum lenght of 50mm including the shaft. The motor must be lightweight, preferably less than 100g. The motor coupled to the mirror must provide a resolution of less than 1 arcsecond	S.L.M.G.

Tabla 3.3: List of demands part 3

3.2.2 Development of the Function Structure

The development of the function structure begins by analyzing and organizing the previously established list of requirements. This process identifies all the functions that the system must perform to achieve its primary objective.

3.2.2.1 Abstraction: Black Box

The Black Box presents an abstract understanding of the system, which separates the sensing devices from the designed mechanical and electronic infrastructure. Figure 3.4 shows the inputs and outputs of the optical alignment process.

It is important to mention that the photon counting data and the simultaneous detection data, i.e., the coincidences, are input signals delivered from an external time tagger device, which is not part of the designed system and therefore cannot be defined with control parameters.

Furthermore, the mirror kinematic mounts are pre-existing commercial components and are not part of the designed system. However, the system developed in this project includes the selection of motors that physically interact with the knobs of these commercial kinematic mounts to automate the alignment of the optical mirror.

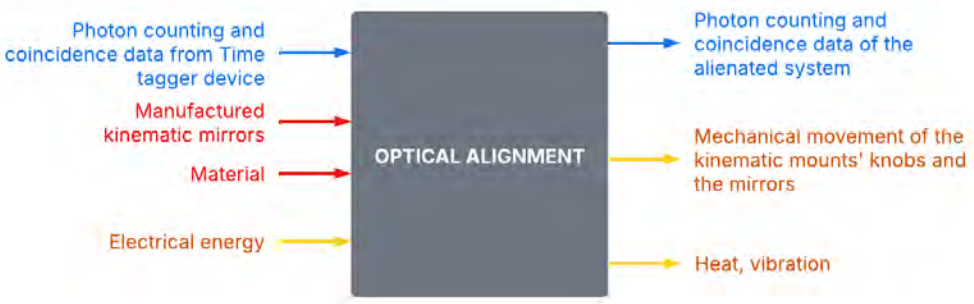

Figure 3.4: Black box for a quantum optical alignment system

3.2.2.2 Function Structure Development

The design of the system control for a quantum entanglement optical alignment system involves the integration of mechanical, electronic, and control components to manage the position of 8 stepper motors, optimizing photon count detection.

The mechanical area consists of three main elements; in figure 3.5 shows this arrangement ensures precise alignment and stability for photon beam manipulation.

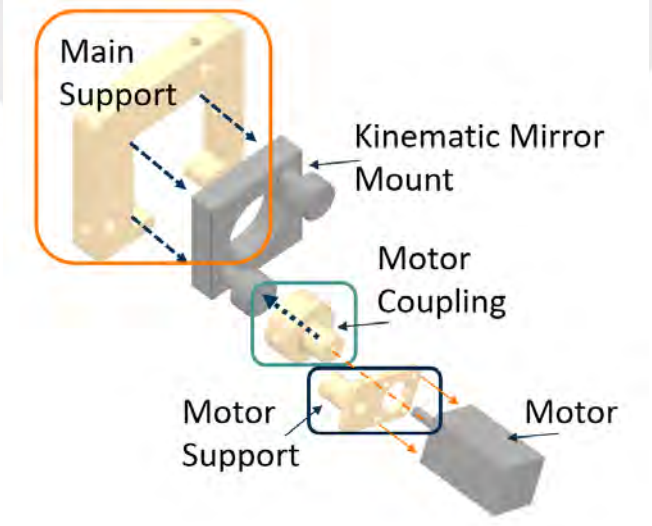

Figure 3.5: Elements in the mechanical area

- **Main Support:** A structure serves as the primary support and is attached to the kinematic

mirror supports.

- **Motor Coupling:** It is the structure that connects the motor shaft to the optical mirror knob.
- **Motor Support:** A structure that holds the motors.

The following figure 3.6 shows the electronic system connections and the control system process.

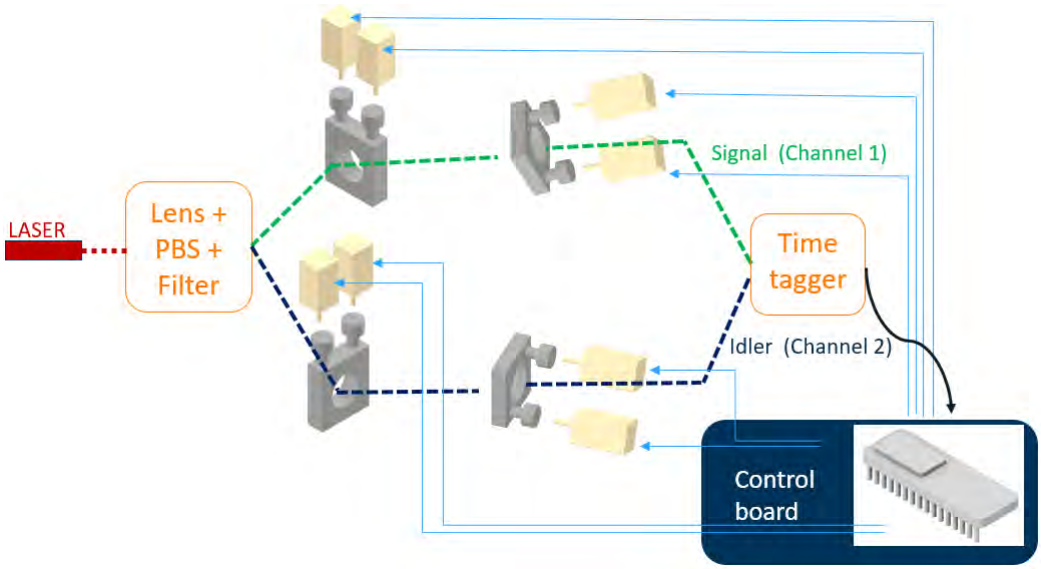

Figure 3.6: Electrical Connections and Data Flow Diagram

The electronic system connects the stepper motors to the drivers on the control board. The sequence of operations is as follows:

- The electronic board is designed, manufactured, and the selected components are soldered.
- The motors are connected by cables to the control board
- The control board regulates the voltage that also power the motors.
- The controller sends commands to rotate the motors clockwise or counterclockwise.
- The controller reads the position information of the motors.

The control system processes and optimizes the motor and detector data by:

- **Filtering Noise:** Removing background noise from the photon detector signals.
- **Photon Signal Analysis:** Monitoring the increase in photon counts and identifying the optimal alignment position where the maximum number of coincidences between the signal and idler photons occur.
- **Storing data:** The number of steps executed by each motor is recorded, along with the data from photon detectors to further analysis.

Since the project is adaptable to the optical alignment of entangled photons, it is considered that it can be replicated in different scenarios where four optical mirrors are used. Therefore, the manufacturing process of the mechanical parts and the electronic card for the alignment control of the optical mirrors are included in the structure function of the figure 3.7.
With the above information, the function structure shown in the figure 3.7 is proposed.

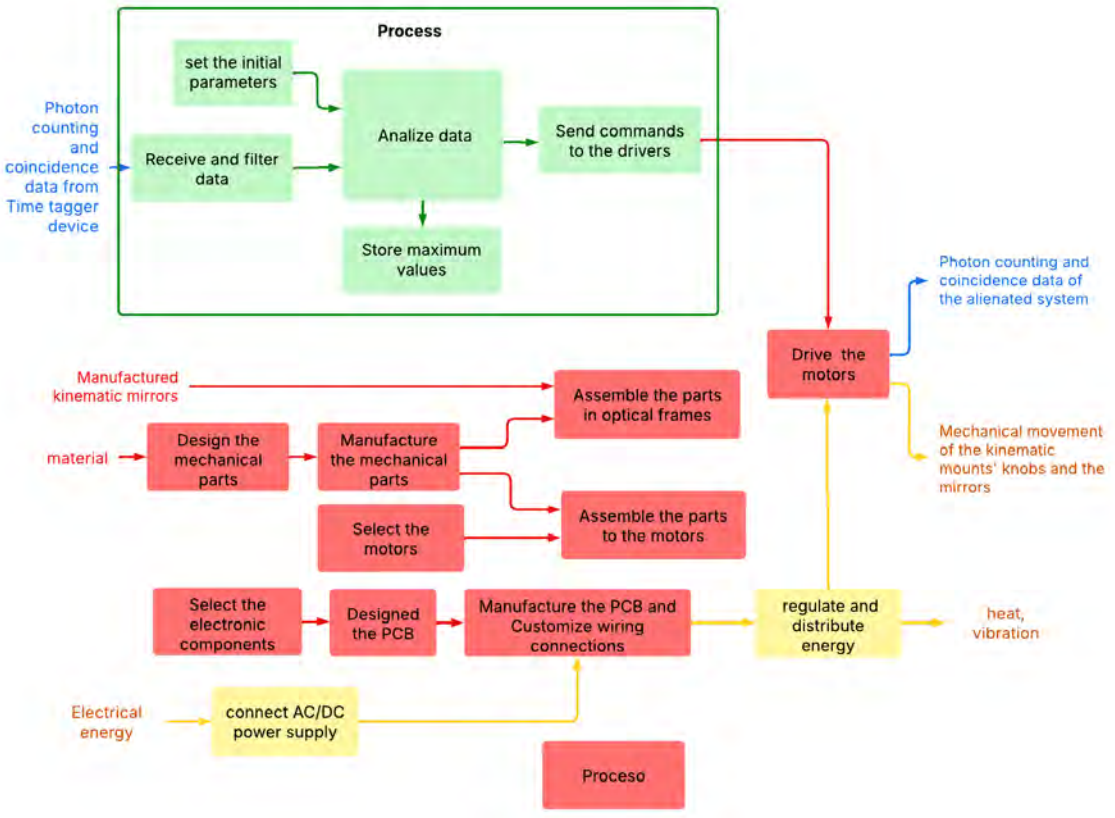

Figure 3.7: Functions Structure for a quantum entanglement optical alignment system

3.2.3 Generation of Alternative Solutions

In this section, the morphological matrices for each domain are presented, which helps to observe different solutions in the electrical, mechanical and control domains.

3.2.3.1 Morphological Matrix by Domain: Electrical

The limited real-life workspace has been taken into account in the project, so the use of small-sized motors is recommended.

The creation of the morphological table for the electrical domain narrows down the options for the most favorable motors due to their size.

The most favorable alternatives for the motors are shown in the table 3.4

	Advantages	**Disadvantages**
Stepper Motors	Compact size. High precision for fine adjustments required in photon alignment. Widely available and cost-effective.	Limited torque, which might require additional support mechanisms depending on the application.
DC Micro Motors with Encoders	Smaller size compared to stepper motors. Encoder feedback allows precise position control.	Requires more complex control systems compared to stepper motors.
Piezoelectric Motors	Extremely small size, ideal for tight spaces. High precision and fast response.	More expensive than stepper or DC motors. They are sensitive and can be damaged with excessive vibration. Designed to handle small loads, so they are less robust for high torque applications.

Tabla 3.4: Favorable alternatives of motors

Considering the motor alternatives given above in the table 3.4 and since external equipment such as the photon detector, which transmits information to the laptop, must be taken into account, the microcontroller must be compatible with the system. It must support fluid communication with the laptop to send and receive data, while providing control signals to the motors. The morphological matrix of the electrical domain is shown below in the table 3.5

Morphological Matrix for Electrical-Electronic Design				
	Alternative 1	**Alternative 2**	**Alternative 3**	**Alternative 4**
Receive, filter and analyze the data				
Send commands to the drivers				
Select the motors				
Drive the motor				
Convert AC/DC				
Regulate energy				
Distribute energy	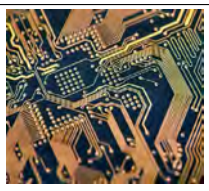	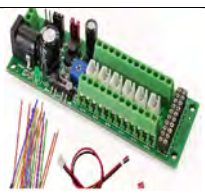		

Tabla 3.5: Morphological matrix for the electrical-electronic domain.

3.2.3.2 Evaluation of sensors, microcontrollers, and actuators

- **Comparison of alternatives to select the motor**

  The main component is the stepper motor which is used to make the movement of the mirror mount knob. As seen in the list of requirements, a stepper motor with a small step angle is required, in addition to a small size due to having a reduced space in which to operate.

  The stepper motor has a resolution of 1.8 degrees per full step, and one full revolution of the adjustment knob tilts the mirror by 0.75 degrees (2700 arcsec). This means that each full step of the motor results in a mirror tilt of 0.00375 degrees (13.5arcsec).

Characteristic	Desired value	Nema17	Nema8 90:1	Nema8	28BYJ-48
Motor type	Bipolar Stepper	Bipolar Stepper	Bipolar Stepper	Bipolar Stepper	Unipolar Stepper
Step Angle	$\leq$ 0.1 deg	1.8 deg	1.8 deg (0.02 deg)	1.8deg (0.1125 deg)	5.6 deg (0.7 deg)
Holding Torque	$\geq$ 3Ncm	13Ncm	1.6Ncm	4Ncm	34Nm
Rated Current/phase	$\leq$ 4A	0,7A	0,6A	0,2A	55mA
Frame Size	$\leq$ 20x20mm	42x42mm	22x22mm	20x20mm	28x35mm
Body Length	$\leq$ 30mm	25mm	38mm	28mm	19mm
Shaft Length	$\leq$ 10mm	20mm	15mm	10mm	10mm
Weight	$\leq$ 100g	180g	130g	60g	33,3g
Price (€)	$\leq$ 30	7,4	48,85	20,8	1.25

Tabla 3.6: Comparison of alternatives to select the motor

A driver will be required to compete with industrialized options, since they achieve a resolution of less than 1 arcsecond.

- **Comparison of alternatives to select the driver** Once the stepper motor is defined, it is possible to select the driver that will be used to control it. Using microstepping with a 1/8 step driver, the effective resolution improves to 0.00046875 degrees per step (1.68749 arcsec) and with 1/16, the resolution will be 0.000234375 degrees per step (0.843749 arcsec). Also, the driver chosen must operate Bipolar Stepper Motors, the options are presented in table 3.7

Characteristic	Desired value	TMC2208	A4988	AMIS -30543	DRV8825
Operating voltage range	$\leq$ 5-24v	5-36V	8-35V	6-30V	8,2v-45V
Max continuous current per phase	$\leq$ 4A	1.4A	1.5A	1.8A	1.5A
Microstepping rating	$\geq$ 16	1-256	1-32	1-128	1-256
Price (€)	$\leq$ 20	3,2	1,1	19,9	18,95

Tabla 3.7: Comparison of alternatives to select the driver

- **Comparison of alternatives to select the microcontroller**

  Each motor driver requires at least 2 pins to control the step and direction of the motor. Consequently, the microcontroller must have a minimum of 32 available input/output pins to accommodate all required connections effectively.

Characteristic	Desired value	Arduino UNO	ESP32	Arduino Mega
Operating voltage range	3v$\leq$ V $\leq$5v	5V	5V	6-30V
I/O	$\geq$ 32	34	14	16
SRAM	$\leq$ 16 MHz	16 MHz	Dual-core processor, each running at up to 240 MHz	16 MHz

Tabla 3.8: Comparison of alternatives to select the controller

The alternatives given in the morphological matrix are analyzed and evaluated. Based on this analysis, the following decisions are presented:

- The simplest and most robust step motors to control are considered (Alternatives 1, 2, and 3), paired with a precise yet easy-to-connect driver (Alternative 2).
- A microcontroller with a minimum of 32 input/output pins and a faster processor (like the ESP32 with 240 MHz) will execute instructions and handle serial data more efficiently. Additionally, serial communication works for sending and receiving data, the transmission speed in bits per second (bps) affects the sending time. Alternative 3 is sufficient with the requirements since it also uses a baud rate of 115200 bps or higher, which is a good option for transmissions in less than 100 ms
- Since the photon detector communicates and transmits data using Python, the data can be read through a Raspberry Pi (Alternative 1) or a laptop (Alternative 2).

- Given the choice of drivers and motors, a power supply exceeding 20A is required, with Alternative 1 being the most recommended.

The yellow solution of Table 3.5 is the most suitable for the system.

3.2.3.3 Morphological Matrix by Domain: Mechanical

The creation of the morphological matrix for the mechanical domain is based on the selection of materials to support the motors and integrate them with the optical kinematic mirror mount. The motor shaft must be coupled to the knob of the optical kinematic mirror mount, ensuring proper alignment and functionality.

Morphological Matrix for Mechanical Design			
	Alternative 1	**Alternative 2**	**Alternative 3**
Design the mechanical parts	AUTODESK FUSION 360	AUTODESK INVENTOR	SolidWorks
Manufacture the mechanical parts	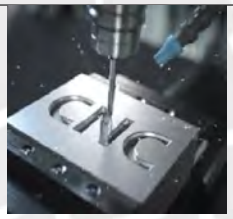	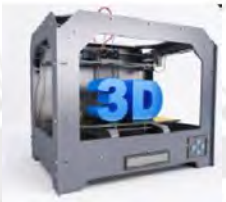	
Assemble the parts in optical frames			
Assemble the parts to the motors			

Tabla 3.9: Morphological matrix for mechanical domain

Since there are two mirrors connected to each optical mirror mount, one on the tilt knob and the other on the tilt axis, it is preferable to have an individual support for each mirror to allow the motor to slide parallel to the axis. Additionally, because the system works with two different optical mirror mounts, a design made from PLA is recommended, as it allows for easy modifications based on the size of the mirror mounts. In this way, the coupling between the motor shaft and the mirror knob should ideally be a single, adaptable piece that fits the radius of the knob. To achieve this, a D-shaped shaft is preferred.

The yellow solution of Table 3.9 is the most suitable for the system.

The system operates with the Radiant Dyes Layer model3.8a, where the motors must be mounted horizontally, and Thor Labs model 3.8b where the motors are mounted vertically. Both kinematic mounts of the optical mirrors are represented in the figure 3.8

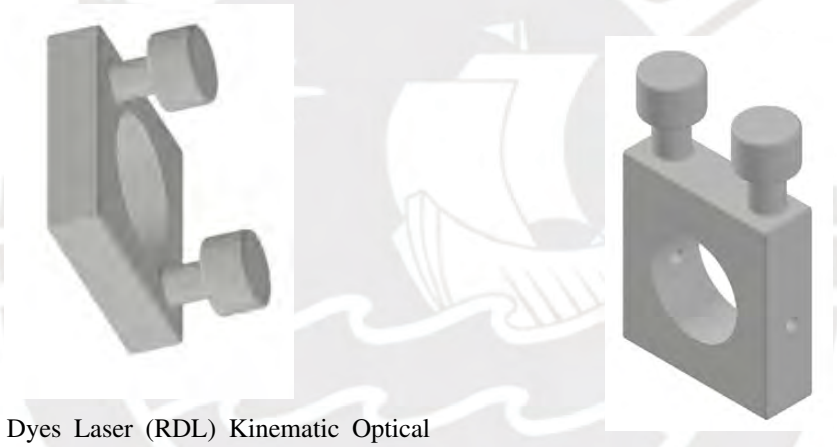

a. Radiant Dyes Laser (RDL) Kinematic Optical Mirror Mount

b. Thor Labs Kinematic Optical Mirror Mount

Figure 3.8: Representation of Kinematic Optical Mirrors

It is observed that the RDL model is the most complex and therefore alternative supports are evaluated and presented in the table 3.10 also presents the evaluation of the shaft coupling design and the motor support design.

Alternatives of the Optimal Integrated Solution			
Component	**Alternative 1**	**Alternative 2**	**Alternative 3**
Main Support for Radiant Dyes Laser Kinematic Optical Mirror	**Asymmetrical Frame** 	**Symmetrical Frame** 	**Symmetrical Frame** 
Step Motor Support	**Asymmetrical** 	**Symmetrical** 	**Symmetrical with pin input** 
Motor Coupling	**Two pieces** 		**One piece for D-shaft** 

Tabla 3.10: Comparison of alternatives to select the general mount

Alternative 3 of Table 3.10 is the most suitable for the system.

3.2.3.4 Morphological Matrix by Domain: Control

The system functions by splitting a photon into signal and idler components, which must then be aligned using two optical mirrors each before being detected by the quTAG detector. The quTAG is a high-precision time-to-digital converter optimized for Time-Correlated Single Photon Counting (TCSPC).

1. **System Inputs and Outputs**

   - **System input (Input):**
     - Photon counting data from Time tagger device: It provides a numerical value that follows a Gaussian distribution where the peak corresponds the highest photon counts values indicating that the mirrors are correctly aligned.
     - Coincidences data from Time tagger device: Value that increases when the mirrors are correctly aligned.
   - **System output (Output):**
     - Photon counting and coincidence data of the alienated system:It represents the received optical intensity and obtains the alignment.

– Motor Step counter: An internal value generated by the software that records the number of steps executed by the motor. It is used as an indirect reference for the motor's position and, therefore, for the mirror's rotation.

2. **Control strategies**

Some control strategies that can be applied to the optical alignment system are presented:

- **Alternative 1: Open loop control**:

  Figure 3.9 shows the system in an open-loop configuration, where the microcontroller control the rotation of the motors, executing the instructions considering a number of motor steps and consequently the motors adjust the mirror position without feedback.

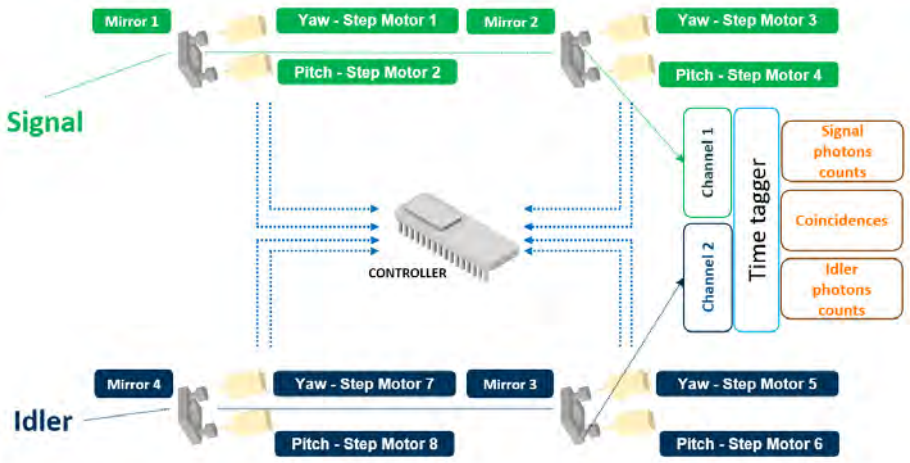

Figure 3.9: Open Loop for a quantum optical alignment system

- **Alternative 2: Control On/Off** There is feedback but the decision is based on whether it is less than or greater than a desired value.
- **Alternative 3: Close loop control (gradient search)**:

  Close loop needs feedback to compare and minimize the error between the actual and desire value. A diagram is shown in figure 3.10. Feedback is obtained by receiving the current values from the time tagger and continuously compares the new signal with the processed and saved values. Since the system resets at each startup and external conditions may change, a basic strategy would be a maximum search algorithm, where:

  (a) A mirror's motor is moved in one direction and the change in signal is measured and recorded.

  (b) Continuously compares each new photon count value with the highest value stored so far.

(c) If the values increases, it continues moving in the same direction.

(d) If the values decreases, the movement is reversed to approach the last known best value.

(e) When the system detects that the data no longer improves within a defined range, it stops the motor, assuming it has reached an optimal or near-optimal point.

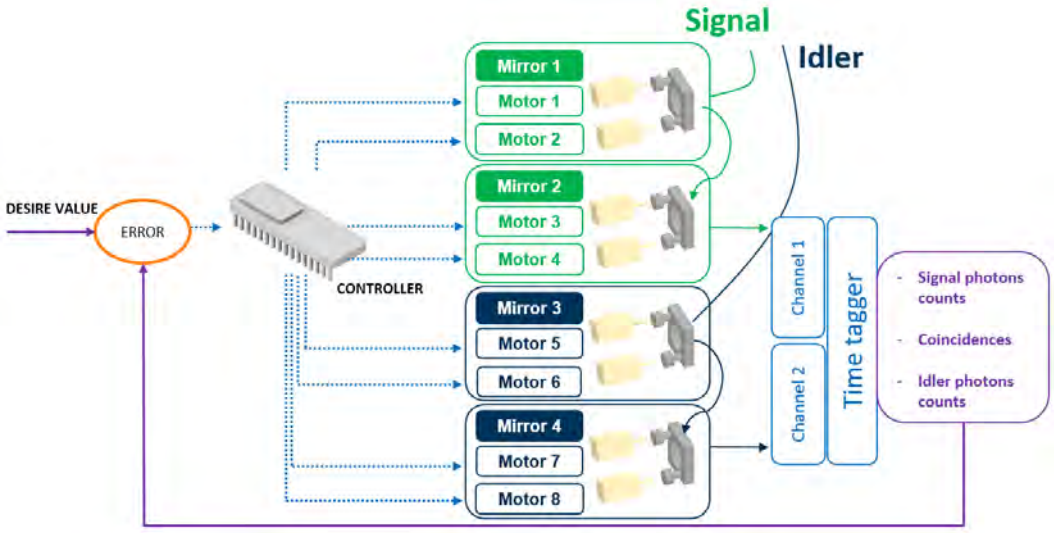

Figure 3.10: Close Loop for a quantum optical alignment system

- **Alternative 4: Control Proporcional-Integral-Derivativo**

  It requires defining a fixed reference and continuously measuring the error between the current output and that reference. It adjusts the motor speed and direction based on that error.

- **Control architecture**

  - **Alternative 1: Local Control with Autonomous Microcontroller:**

    All processing and decision commands would occur within the microcontroller. An advantage would be low power consumption and a disadvantage would be limited processing capacity.

  - **Alternative 2: Master - Slave Control**

    Control and communication systems where one device (the master) has centralized control and one or more devices (the slaves) follow its orders.

    * **Master:** It is responsible for coordinating communication and decision making. It sends commands to the slaves and receives responses.

    * **Slave:** They carry out the master's orders, and respond the master when it is consulted, but cannot initiate communication on their own.

Since the project must include the laptop to run the time tagger software, it is convenient to centralize the processing, becoming the master, in this way, advanced analysis would be performed in Python without depending on the computational capacity of the microcontroller.

The microcontroller, being the slave, responds to the master's instructions and is only responsible for controlling the movement of the motors.

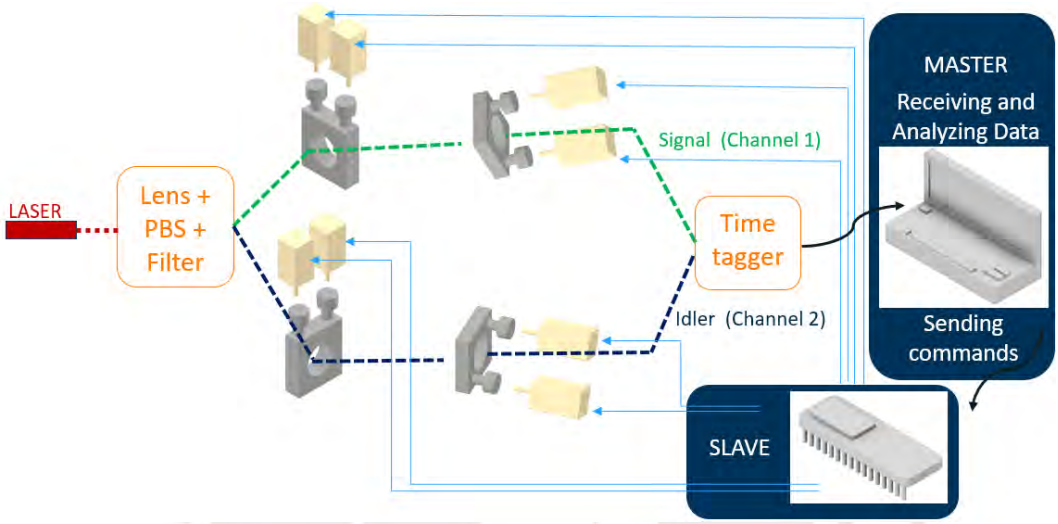

Figure 3.11: Master - Slave control for a quantum optical alignment system

The detected signal is highly sensitive to small variations in light intensity. It is recommended to filter the signal before processing it as a reference. Furthermore, because of these subtle changes, it is advisable to analyze whether the overall trend of the data indicates an increase or not.

3.2.4 Optimal Integrated Solution Concept

Since the QuTAG device operates with Python libraries, it simplifies integration with microcontrollers that can also be programmed using Python. This compatibility allows communication and control within the same software environment, streamlining overall system development.

After evaluating various alternatives in the mechanical, electrical and control domains, these options were integrated to provide different system configurations. Among these, the most suitable alternatives are presented in Table 3.11.

- **Alternative 1:** A Nema 17 stepper motor is used, which offers the advantage of greater torque. However, it has drawbacks, such as higher power consumption and larger size. Due to motor's weight, it is recommended to use metallic materials for the motor support with a robust structural design, which must also be anchored to the table holding the optical mirrors. This increases the required workspace and can interfere with the precise alignment of the

Alternatives of the Optimal Integrated Solution		
Alternative 1	**Alternative 2**	**Alternative 3**
	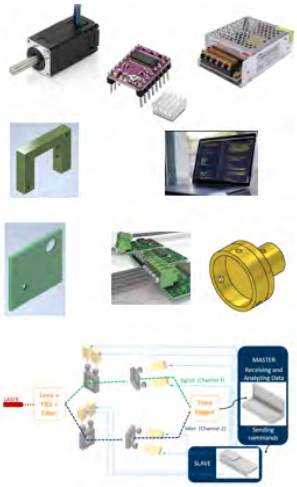	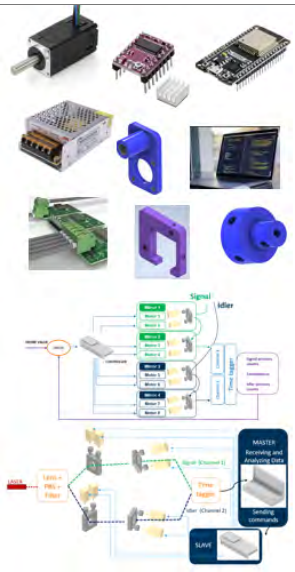

Tabla 3.11: Alternatives of the Optimal Integrated Solution Concept

photon beams. Furthermore, using an open loop control would take longer for alignment compared to other controls.

- **Alternative 2:** A Nema 8 stepper motor is used, controlled by mid-range drivers capable of dissipating heat through small heatsinks. These motors can be powered by a 9-12V power source, which is easy to find, and the cables used must support currents of up to 1.5A. In addition, it is recommended to use a power supply with a minimum capacity of 25A to reliably power all 8 motors in parallel. A metal casing is ideal as it efficiently dissipates heat, reducing the risk of overheating and enhancing the power supply's performance and longevity. The compact size of the motors Nema 8 allows to use PLA material to construct their support, allowing for an asymmetric design tailored to the specific mounting requirements. Also, closed loop control reduces the error between a reference and the current data reading given by the time tagger, but it must be taken into account that even if there are no changes in the motor positions, the value may vary and therefore it may be difficult to set a reference as the desired value.

- **Alternative 3:** This option is similar to Alternative 2 but uses a generalized symmetric design that can adapt to different optical mirror setups without requiring significant changes to dimensions. This flexibility makes it an optimal choice for the systems that require frequent adjustments or adaptations. In addition, a master-slave architecture is efficient because it takes advantage of the processing power of the laptop and the ability of the ESP32 to control the movements of the motors. And the control becomes more robust if combined with

closed-loop.

3.2.5 Technical and Economic Evaluation of the Design

The next step according to the referential design regulations is to analyze the alternative solutions proposed. Therefore, both technical and economic general criteria will be taken into account for each solution alternative, and it should be noted that the calculation is obtained from the sum of the values.

Technical evaluation of the project				
Project: Design of the system Control for a quantum optical alignment system				
The score range is between 0 and 4. 0 = Does not satisfy, 1 = Acceptable, 2 = Enough, 3 = Good, 4 = Very good				
No.	**Technical criteria**	**Solutions**		
		1	**2**	**3**
T1	Good use of energy	1	4	4
T2	Rigidity	4	3	3
T3	Security	3	3	4
T4	Speed	1	3	4
T5	Stability	1	3	4
T6	Transportability	1	2	4
T7	Quality of work	2	4	4
T8	List of demands	1	2	4
	Total sum of technical evaluation	14	24	**31**

Tabla 3.12: Technical evaluation for electrical-electronic and mechanical design

Economic evaluation of the project				
Project: Design of the system Control for a quantum optical alignment system				
The score range is between 0 and 4. 0 = Does not satisfy, 1 = Acceptable, 2 = Enough, 3 = Good, 4 = Very good (ideal)				
No.	**Economic criteria**	**Alternatives**		
		1	**2**	**3**
E1	Number of pieces	1	4	4
E2	Easy acquisition of materials	4	1	3
E3	Productivity	1	3	4
E4	Diverse costs	1	3	4
E5	Ease of assembly	1	2	3
E6	Ease of maintenance	1	3	4
	Total sum of economic evaluation	9	16	**22**

Tabla 3.13: Economic evaluation for electrical-electronic and mechanical design

From the technical-economic criteria, the third optimal integrated solution alternative was chosen, which consists of using an ESP32 control card, likewise, the gearless Nema 8 stepper motors and the A4988 drivers that will allow to have a 16:1 step reduction.

After comparing various options, the decision was made to use a NEMA 8 stepper motor without an integrated reducer, paired with A4988 drivers, and controlled by an ESP32 microcontroller.
The NEMA 8 stepper motor is suitable for applications that require compact size and moderate power. It works effectively with midrange A4988 drivers, which are capable of managing heat dissipation through a small heatsink. These motors are powered using a standard 9-12V power supply, which is readily available. In addition, the wiring connecting the motors must be able to handle currents up to 1.5A to ensure reliable operation.

3.3 Preparation of the final design

3.3.1 Electronic design: Initial Design Approach and Evolution to the Final PCB

- **Stage 1: Initial Cable Setup**

  The initial prototype, shown in Figure 3.12a used individual off-the-shelf components connected via separate wires, due to their ease of access and the convenience of replacing any failed components during early testing. This approach allowed for rapid prototyping and ensured that any issues could be addressed by simply substituting faulty parts without requiring significant redesign.

- **Stage 2: Shield PCB for Testing**

  To overcome the issues of the first stage, a shield PCB, shown in Figure 3.12b was designed to act as a bridge between the components. This intermediate design significantly reduced cabling and improved organization, making testing more efficient while still allowing flexibility for adjustments. (Include photo of the shield PCB setup.)

- **Stage 3: Final Integrated PCB**

  Once the testing phase was completed, the final PCB design was optimized by integrating the drivers, resistors, and capacitors into a single, cohesive board. This integration eliminated unnecessary wiring, reduced noise, and enhanced the robustness of the system, all while retaining the functionality of the A4988 drivers and the ESP32 microcontroller, the final design achieved a streamlined and reliable solution, minimizing external dependencies and optimizing performance.

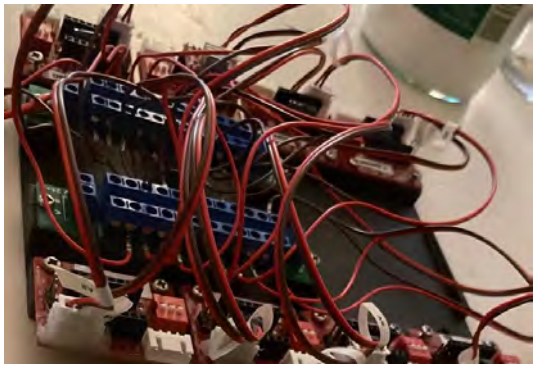

a. Photo of System Assembly with 3D Wiring and Support - Initial Setup for testing

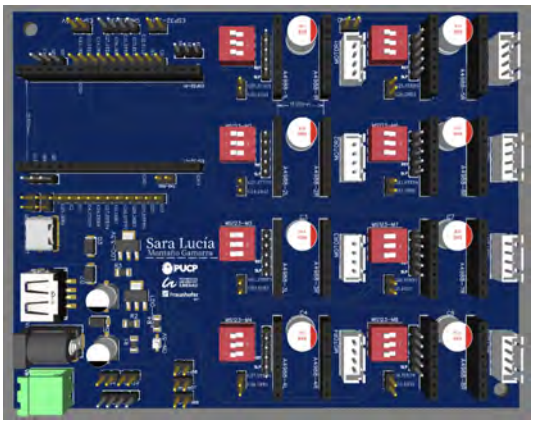

b. 3D View of Electronic Design in EasyEDA - Shield PCB for testing

Figure 3.12: Evolution of the PCB Design

3.3.2 Electronic design: Description of the final circuit schematic

The figure 3.15 show the final design of the electronic board for quantum optical alignment control that incorporates the ESP32-WROOM-32UE microcontroller with 16MB of flash memory. The board is powered via a USB-C connection and communicates digitally with 32 pins connected to 8 A4988 motor drivers, which manage the step and direction signals for the motors. Additionally, the board uses 4 digital pins to enable the motors in pairs, as each optical mirror is adjusted by two motors connected in parallel.

The motors are powered by a 12V power supply,while the drivers receive their digital voltage of 3.3V through the AMS1117 - 3.3 voltage regulator. This design ensures precise motor control and efficient power distribution for the quantum optical alignment system.

Following the typical application diagram provided in the A4988 datasheet, the following connections are made:

- Decoupling capacitors for VMOT (12V):
  - C6 capacitor of 4.7 µF capacitor for decoupling.
  - C7 capacitor of 100 nF ceramic capacitor for filtering high-frequency noise.
  - Additionally, a C1 capacitor of 100 µF is added to provide further stabilization of the motor power supply.
- Decoupling capacitor for VDD (logic power supply):
  - C5 capacitor of 220 nF capacitor to stabilize the logic voltage.

- Charge pump capacitors:
  - Between the charge pump pins CP1 and CP2, a C3 capacitor of 100 nF is placed to ensure proper operation of the internal charge pump circuitry.
- SENSE pins and RSense resistors:
  - The SENSEx pins are connected to the RSense (R1 and R3) resistors of $50m\ \Omega$. This minimizes noise and ensures accurate current sensing.
- VREG pin:
  - This pin is decoupled using a C4 ceramic capacitor with a value of 0.22 µF, connected to ground.
  - A R4 resistor of $10k\ \Omega$. is utilized to stabilize the voltage and ensure proper operation.
- Microstepping control:
  - The microstepping control pins MS1, MS2, and MS3 are each connected to an individual switch. The logic level (HIGH or LOW) is determined by the position of the respective switch, allowing manual configuration of the microstepping mode.
- Motor Coil control:
  - The motor coils, corresponding to the output pins OUT1A, OUT1B, OUT2A, and OUT2B, are connected via a Molex connector for secure and reliable connections.
- DIR and STEP:
  - The DIR (direction) and STEP pins are connected directly to the microcontroller, enabling digital control of the motor's direction and step signals.

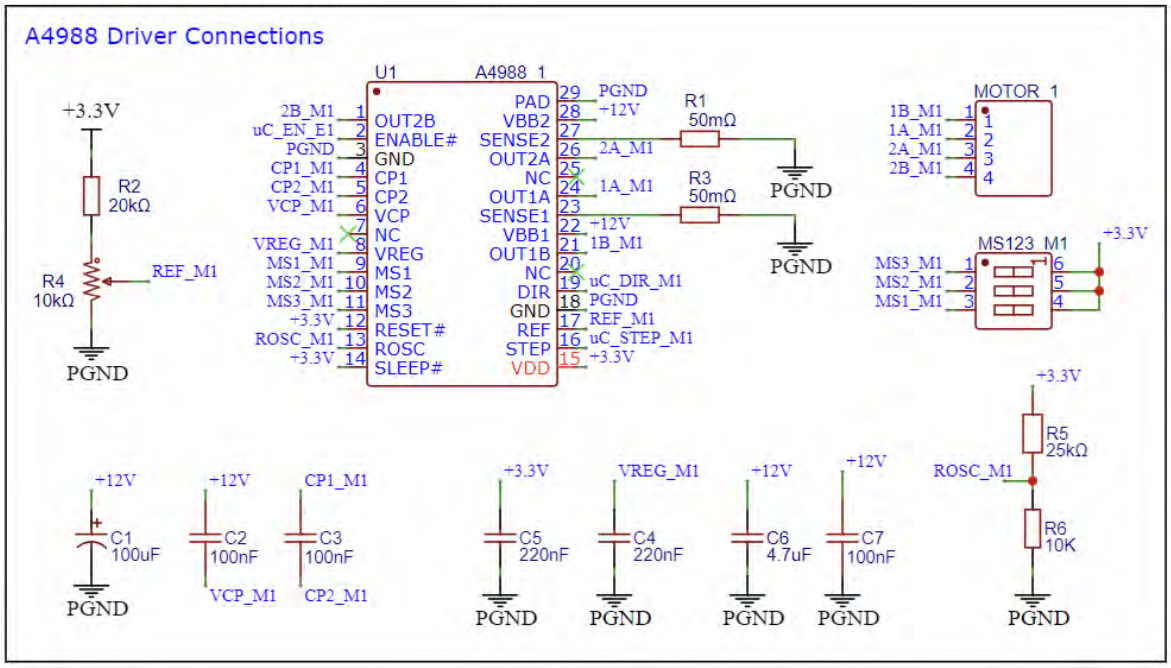

Figure 3.13: Circuit Schematic According to A4988 Datasheet Specifications [29]"

The previous schematic for the A4988 driver in the figure 3.13 is replicated 8 times, with each module connected to the microcontroller via the DIR and STEP pins. Additionally, a decoupling capacitor C57 of 100 nF is included for each driver.

For the USB Type-C converter that powers the microcontroller, the CH340E is utilized, and the USB Type-C connections are detailed in the schematic. This section also includes a power indicator LED, labeled PWR2.

Two buttons are added for the microcontroller: BOOT (SW2) and EN (SW1), used for programming and enabling functions.

The schematic also presents the connections for the 12V power supply, which includes a decoupling capacitor C58 of 4.7 µF and a filtering capacitor C59 of 100 nF. Another power indicator LED, labeled PWR1, is included for monitoring the 12V supply.

Finally, the AMS1117-3.3 voltage regulator is used to step down the 12V input to 3.3V, which is required to power the drivers.

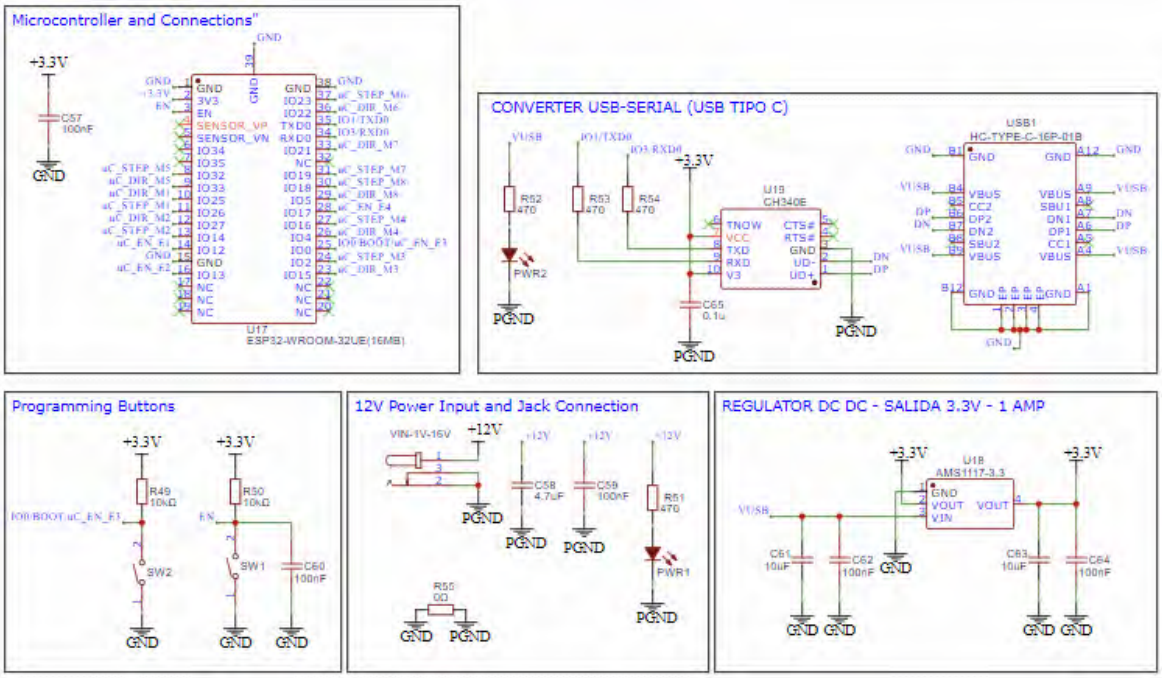

Figure 3.14: Schematic Design Based on Datasheets with Custom Configuration

Figure 3.15 show the 3D model of the circuit generated in EasyEDA, based on the schematics of the datasheet with custom design of the placement of components, connections and routing. The PCB layout is organized into distinct sections to simplify troubleshooting and assembly:

- Microcontroller Section: Includes the ESP32 module and its associated connections, programming buttons, and power input.
- Motor Driver Section: Features 8 A4988 driver modules, each with decoupling capacitors and connections for DIR and STEP signals.
- Power Supply Section: Contains the USB Type-C input, CH340E USB-to-serial converter, AMS1117-3.3 voltage regulator, and capacitors for filtering and decoupling.
- Indicator Section: Includes LEDs PWR1 and PWR2 to indicate the status of the 12V and 3.3V power supplies, respectively.
- 12V Input Section: Features the DC jack and associated capacitors (C58 and C59) to filter and stabilize the input voltage.

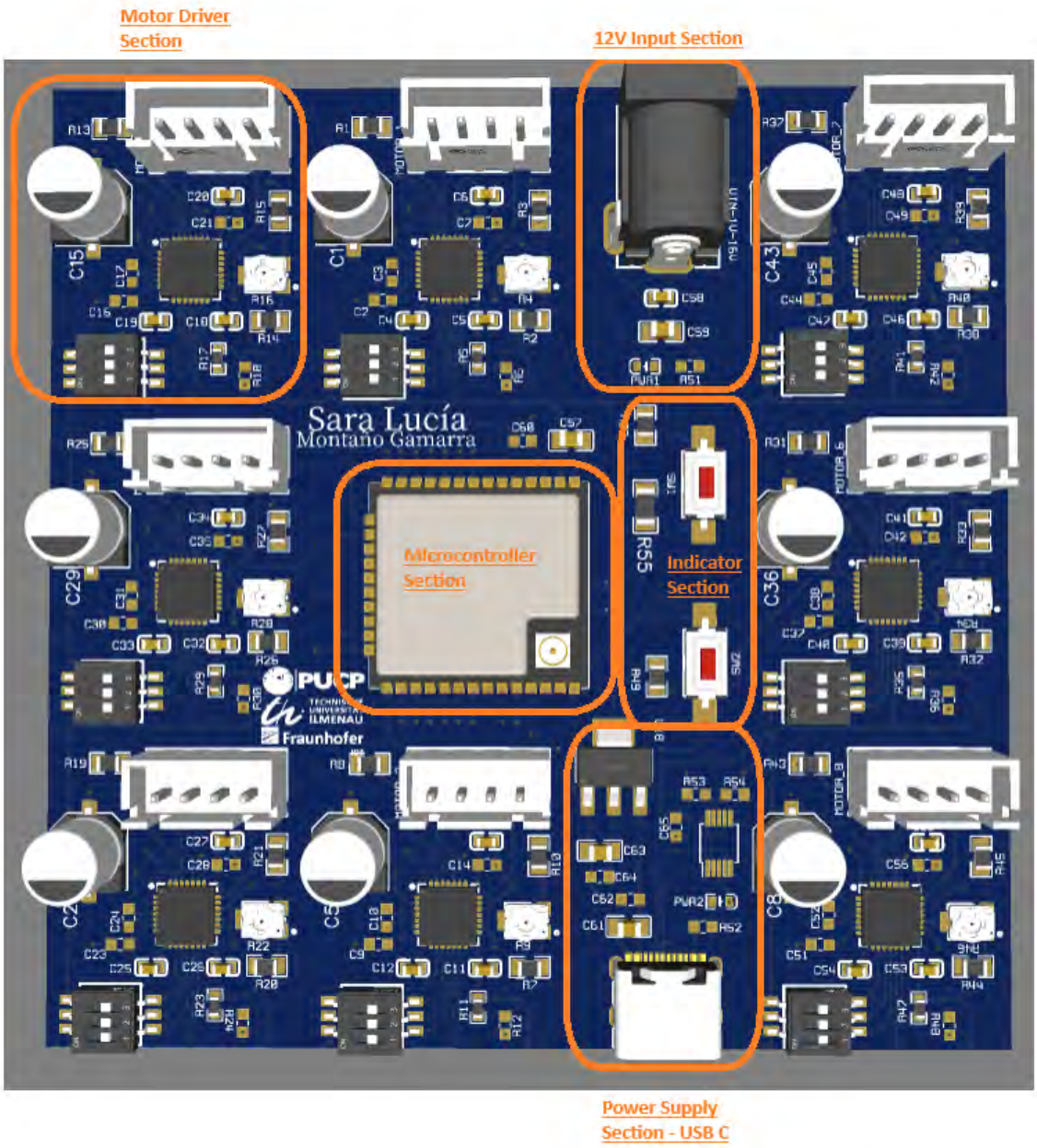

Figure 3.15: 3D View of the Circuit Designed in EasyEDA, Based on Datasheets with Custom Component Placement and Routing"

The PCB consists of four layers:

- Top Layer and Bottom Layer are the Signal Layer: Contains the main traces for data signals, including the connections for the microcontroller, drivers, and peripherals such as buttons and LEDs.
- Middle Layers (Ground and Power Layer): Primarily used for ground planes and power distribution to minimize noise and ensure stable operation.

3.3.3 Mechanical design: Description of modeled parts

- **Main support**

  The system includes two different Two-Point kinematic mirror mounts, making the design adaptable to both types. This support uses PLA material and is designed to hold two motors. The main support, which can be attached to the mirror mount, connects to the individual motor mount via a cylindrical metal pin. It is designed to bear the weight of the stepper motors and ensure the alignment of the motor shafts with the center of the mirror mount knobs.

  It has been designed to be able to adapt to the position of the optical mirror mount, in this way, it is possible to place it on the work table in the most optimal way that helps to optimize space. The first design of the main support is versatile, allowing it to be attached to any side of the kinematic optical mirror mount that has been previously installed. The second design is for a vertical drive optical mount, intended to be positioned on the top part. Both models are secured to one side of the mirror mount using M4 screws.

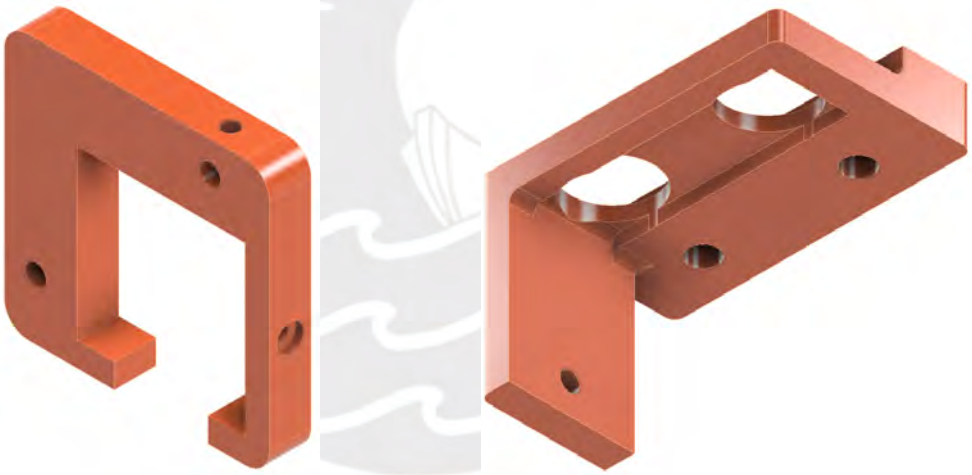

a. Main Support for Radiant Dyes Laser Kinematic Optical Mirror

b. Main Support for Thor Labs Kinematic Optical Mirror

Figure 3.16: Main Supports for Kinematic Optical Mirrors

- **D-Shaft Motor Coupling**

  The adapter attaches to the mirror mount knob with two M3 screws and also attaches to the D-shaped motor shaft with M3 screws.

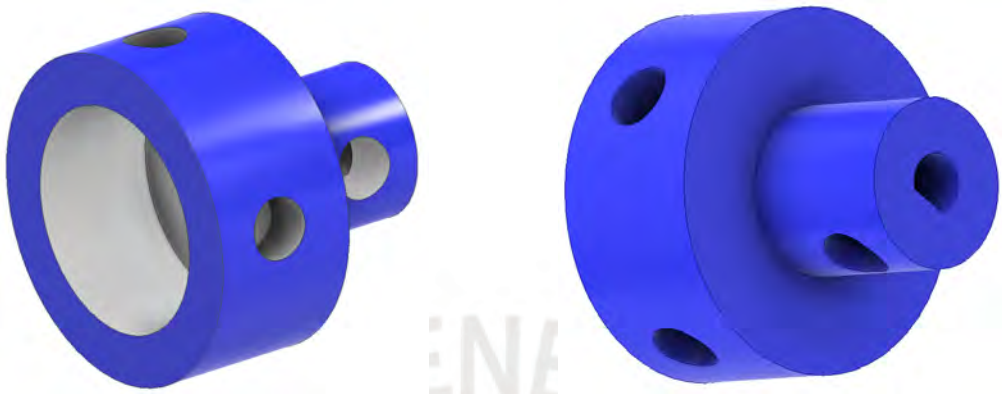

a. Motor Coupling – Knob Optical Mirror's View b. Motor Coupling – Shaft Motor's View

Figure 3.17: D-Shaft Motor Coupling design

- **Step Motor Support**

  The stepper motor mount allows you to screw the 4 M2 screws to fix the motor and also insert the cylindrical metal pin.

  The cylindrical metal pin would be free on the motor mount, which allows for the forward and backward sliding that is generated by turning the optical mirror knobs.

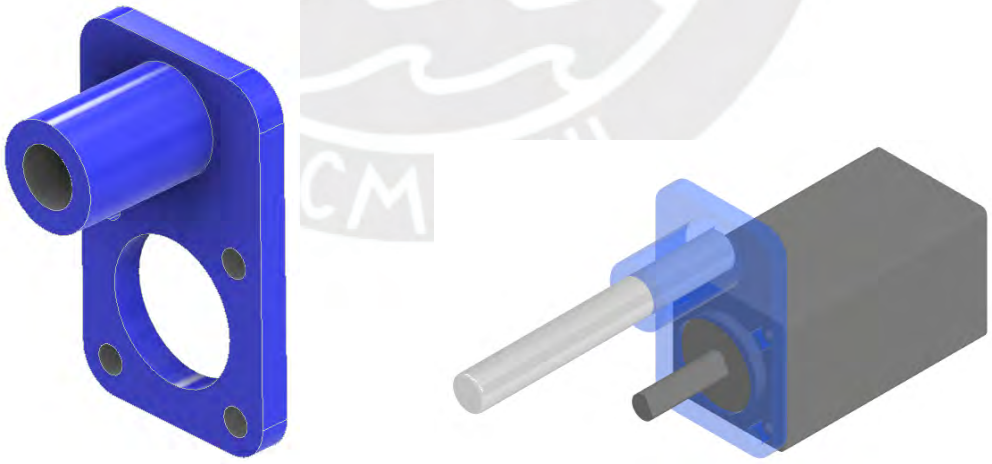

a. Step motor Support b. Motor Mount assembly

Figure 3.18: Step Motor Support design

3.4 Controller design

The peak detection method was chosen based on the nature of the optical alignment system, when the mirror is properly aligned, the system detects a maximum in the photon count.

The system operates as a closed-loop control mechanism, continuously adjusting the motors based on feedback obtained from photon counts detected at 100 ms intervals. These values are continuously compared with the previously recorded maximum value to determine whether the photon count value is increasing or decreasing. Each photon pair, signal and idler, is processed independently but follows the same control strategy.

3.4.1 Peak Detection and Control Strategy

The signal obtained from the photon-counting detector follows a Gaussian-like distribution, with the peak representing the optimal alignment of the mirrors. However, due to the signal's high sensitivity to light, it exhibited significant noise even without moving the mirrors. To address this, the control strategy was designed as follows:

1. **Signal Simulation with Noise:**

   The Gaussian signal created in C++ and programmed in an ESP32 simulating the behavior of a photon detector used in the laboratory.

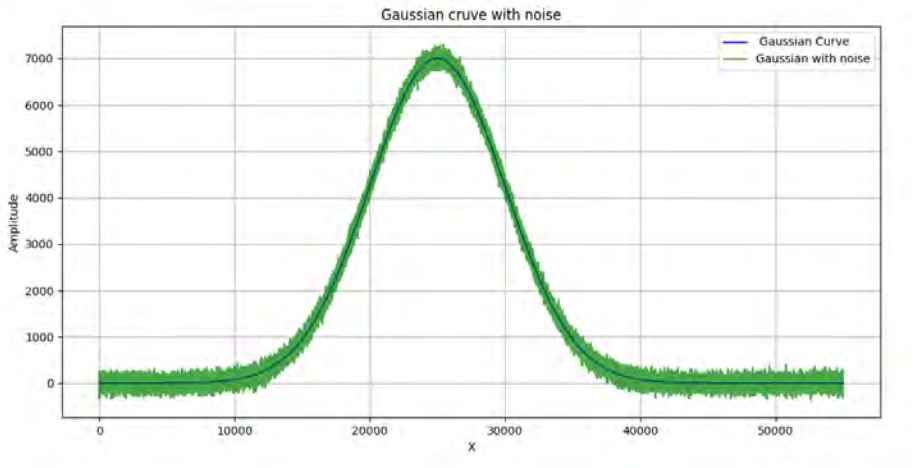

Figure 3.19: (a) Full View of the Simulated Signal. The behavior of the real signal follows a Gaussian curve with noise.

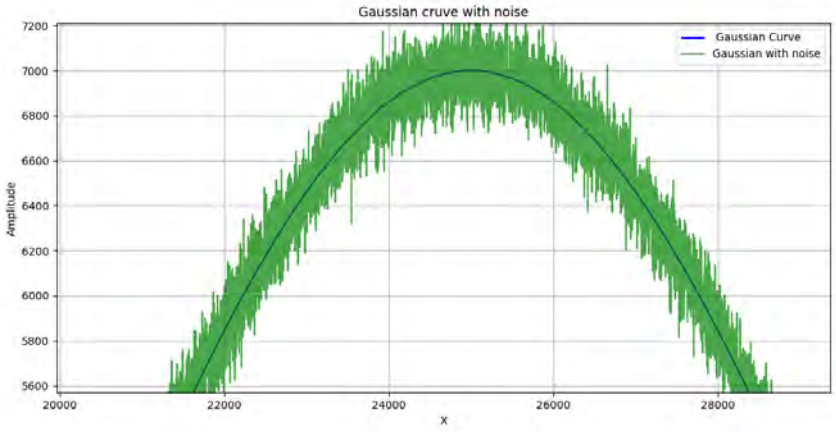

Figure 3.20: (b) Close-Up of the Signal with Noise. A zoomed-in view to illustrate the effects of fluctuations.

2. **Filtering and Smoothing:**

   A low pass filter was integrated into the control logic to reduce noise before controlling the motors, to have better .

   The figure 3.21 shows the results of the filtering applied to the simulated data with noise.

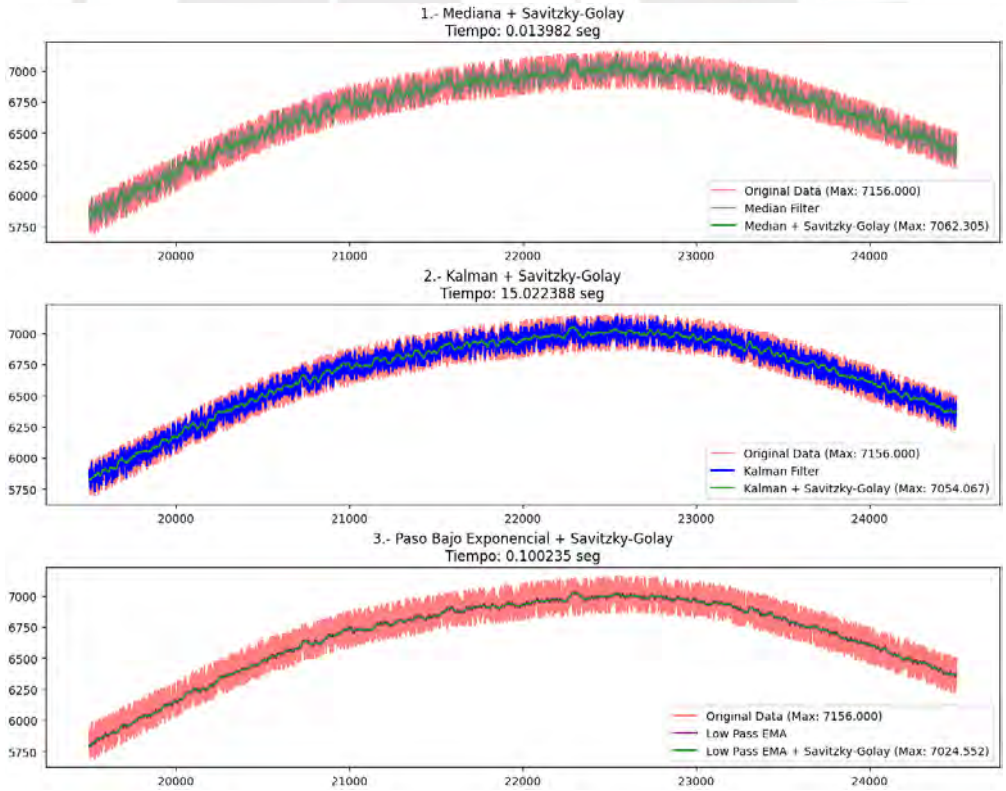

Figure 3.21: Results of the filtering

The filter selection was based on comparing different combinations of Median, Kalman, and

EMA filters, focusing on the range near the highest point of the curve. A window size of 5000 was chosen for analysis.

The results show that applying only the Median filter leaves significant noise, making it necessary to use a smoothing method. While the Kalman filter provides good results, its processing time exceeds 15 seconds, making it unsuitable for our process. The best results were obtained using only the EMA filter, as it effectively reduces noise while maintaining a reasonable processing time. However, it also produces the lowest peak value among the tested filters.

For reference, the original data has a peak value of 71,566. The Median + Savitzky-Golay combination results in 7,062, while the EMA filter achieves 7,024.

3. **Trend Analysis for Motor Control:**

   - **Trend Analysis:** The last 30 data points (or fewer, if unavailable) are analyzed. This analysis evaluates the trend in the photon count (from either the signal or idler detector) over time using linear or weighted regression techniques. The system uses the absolute value of the slope to decide if the trend is strong enough to matter, this ignore fluctuations or noise values. However, the positive sign or the negative sign of the slope is still used to determine direction, classifying as Increasing or Decreasing; otherwise, as No clear trend.
   - **Robust Trend Detection:** Multiple independent methods—including standard and weighted regression, moving averages, and percentage change calculations—are used to confirm the trend. A trend is considered valid if the majority of these methods , at least 3 out of 5, agree on the same direction.
   - **Peak Identification of the photon count values:** Trends are grouped into sets of five consecutive results and compared to predefined patterns. A sequence of Increasing trends followed by Decreasing trends indicates that a peak has been crossed. This approach ensures reliable peak detection by minimizing noise interference and reducing false positives.

4. **Motor Movement logic:**

   - Two motors were linked to control the tilt (til) and rotation (dil) of the mirror.
   - One motor rotates clockwise from the initial position.
   - Continuous data analysis via Python analyzes the trend of the photon counts. If the photon counts increase, the motor continued moving to the right. If the trend is no longer

increasing, the ESP32 controller is instructed to reverse the motor's direction until it detects the maximum value of the photon counts previously found.

3.4.2 Justification of Closed Loop Control

Initially, the goal was to estimate a global model of the system using all available data, consisting of 8 motor as inputs and 3 outputs, the photon count values from the two correlated photons of an entangled pair (signal and idler) and their coincidence counts. This would have enabled a more accurate and coherent representation of the system as a whole. However, due to experimental constraints, such as the inability to obtain certain data, this modeling strategy could not be implemented effectively.

Although the system is inherently MIMO, the alignment strategy was developed through simulations using a simplified SISO approach. Each SISO model considers the effect of a single motor on the corresponding photon count. As previously described, each detection channel (signal or idler) is influenced by four motors.

1. **Continuous Feedback and automatic Correction:**
    - The system continuously analyzes the photon count values from a single detection channel (either signal or idler photon count values) in real time and adjusts the corresponding motor connected to that channel.
    - The direction of movement of the motor is modified based on the trend (increasing or decreasing) of the photon counts.
    - When the system detects a continuously decreasing or unclear trend, it means that the motor is moving away from the maximum value (the alignment point) found previously. Therefore, it will correct the direction of rotation of the motor.
2. **Error Minimization and motor stopping criterion:**
    - In order to avoid false positives caused by noise or fluctuations, the system does not make decisions based on a single photon count value. Instead, the photon count values, either from the signal or idler channel, which behave similarly, are grouped into data windows of 20 to 30 values. Each window is analyzed to determine a majority trend (increasing, decreasing, or unclear), and this information is stored over time to detect real directional changes.

Figure 3.22 shows the behavior of the photon count values without moving the optical mirror. Even if the mirror remains at the same angular position, the photon signal fluctuates naturally.

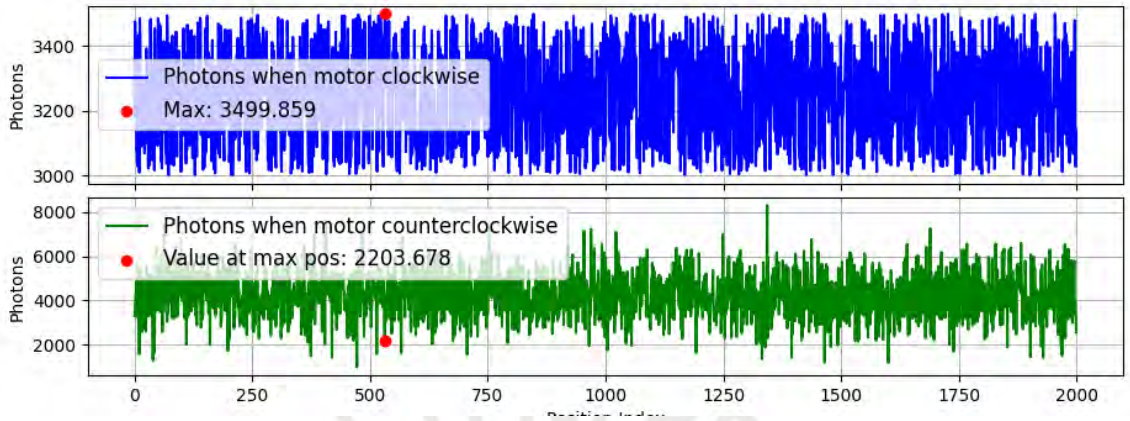

Figure 3.22: Analysis of data of photon counts in the same position index of the motor step

- Therefore, the system defines a range around the maximum, rather than a single value, and uses trend pattern recognition to determine when the motor is approaching or leaving that range. Only when a consistent decreasing trend is detected across multiple windows does the system reverse the motor direction, ensuring alignment decisions are based on robust patterns, not isolated fluctuations.

3.5 System assembly and implementation

- **Preparation**

  i. Place the general motor support in the optical mirror mount.

  ii. Place the metal cylindrical pins to the general support and tighten its screws.

  iii. Attach the D-Shaft motor coupling to the knobs of the kinematic optical mirror mount.

  iv. Position the step motor support and secure it with its four screws.

  v. Fasten the D-Shaft motor coupling to the motors and tight its screw.

  vi. Check the electronic connections of the components to the electronic card.

  vii. Check the connection with the time tagger device designed for time correlated single photon counting.

  viii. Ensure the correct power feeding of the design of the system control.

- **Performance**

  i. Rotate each motor one by one.

  ii. Record the values given by the time tagger.

  iii. Compare in real time the number of singles and idler counts and the coincidences measurements detected by the time tagger.

  iv. Associate the position of each motor with the received values.

  v. Decide the next motor movement and send the information to the control unit.

- **Control**

  i. Check for no error connection.

  ii. Set the position of each stepper motor as a reference for the control unit.

  iii. Decide if the given data by the time tagger is increasing or decreasing.

  iv. Generate a signal (via the control unit) that causes the movements of the motors in the desired direction.

  v. Change the direction of the motors when the values are decreasing.

  vi. Stop the motors when find the peak desire value.

- **Final phase**

  i. Save the position data of the motors for future comparison.

  ii. Repeat the sequence of steps for the operation in case a new setup system misaligned.

In figure 3.23, the 3D mechanical design is shown with its parts separated but arranged for assembly. Also, it can be observed that the main Support for radiant-dyes Laser-kinematic Optical Mirror can be adjusted to fit the mirror's position.

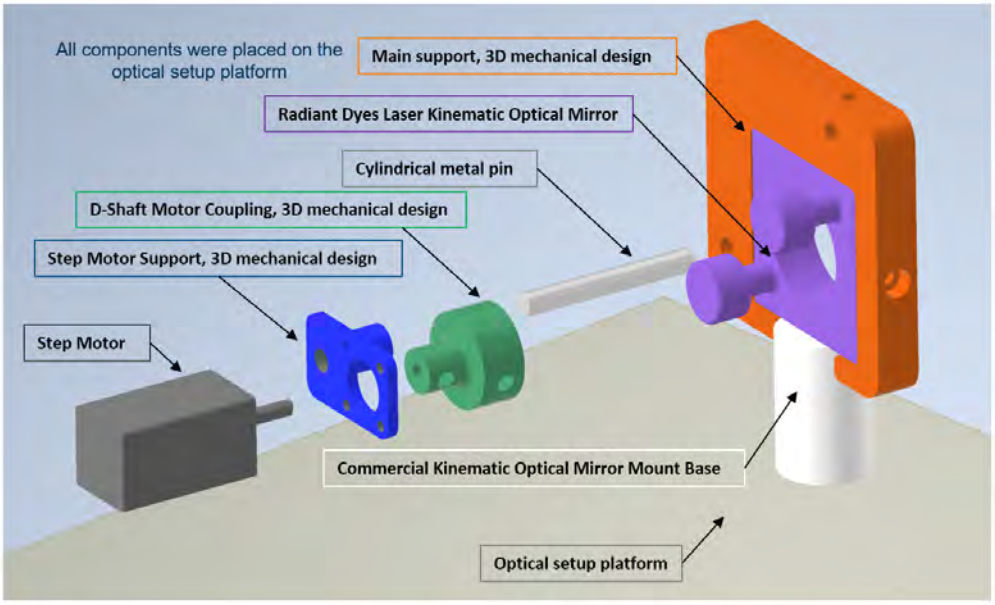

Figure 3.23: Exploded view of the mechanical system for Radiant Dyes Laser Kinematic Optical Mirror

The figure 3.24, shows the system assembled on the Radiant Dyes Laser kinematic optical mount. It can be observed that the mechanical design adapts to the mirror's position, allowing the support to be placed in different orientations as needed.

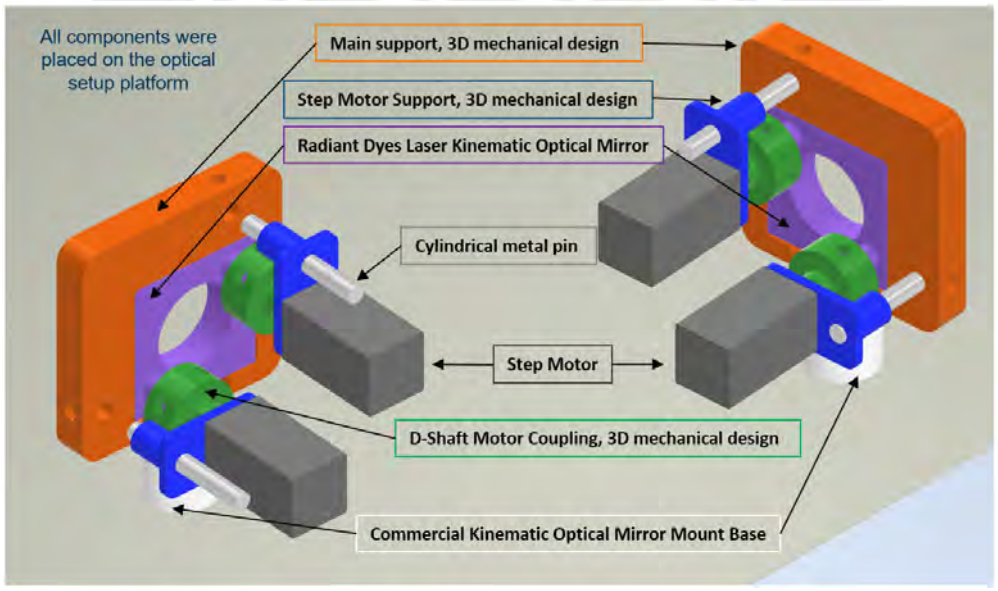

Figure 3.24: Assembled system mounted on Radiant Dyes Laser Kinematic Optical Mirror

In Figure 3.25, the system is shown with its parts separated but arranged for assembly with the Thorlabs Kinematic Optical Mirror.

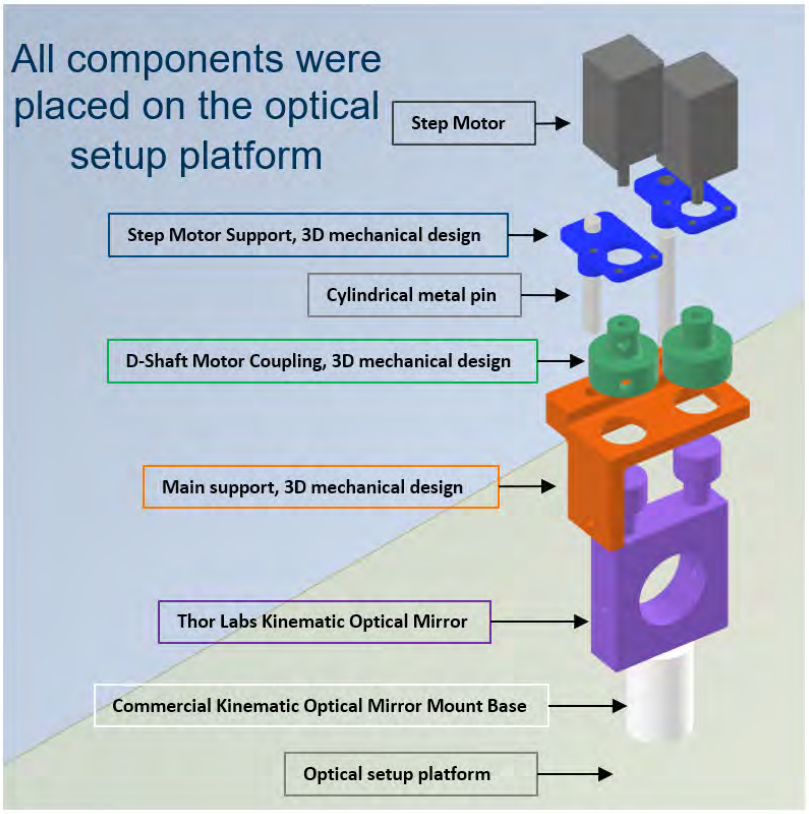

Figure 3.25: Exploded view of the mechanical system for the Thorlabs Kinematic Optical Mirror.

The assembled system using the Thorlabs Kinematic Optical Mirror is shown in Figure 3.26.

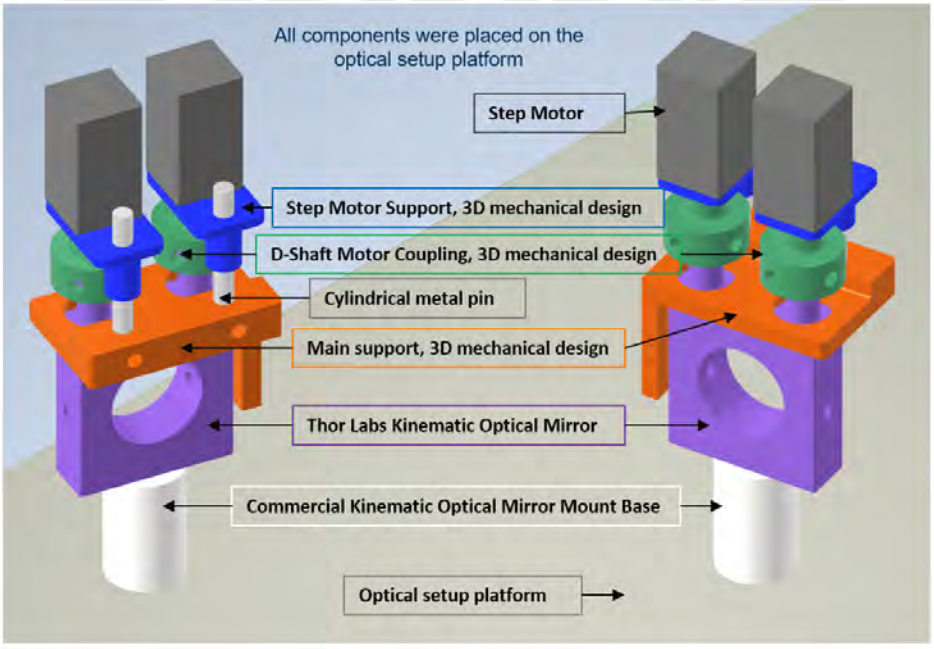

Figure 3.26: Assembled system mounted on the Thorlabs Kinematic Optical Mirror.

Finally, the assembled design of the control system for a set of quantum entanglement optical alignment system is shown in figure 3.27

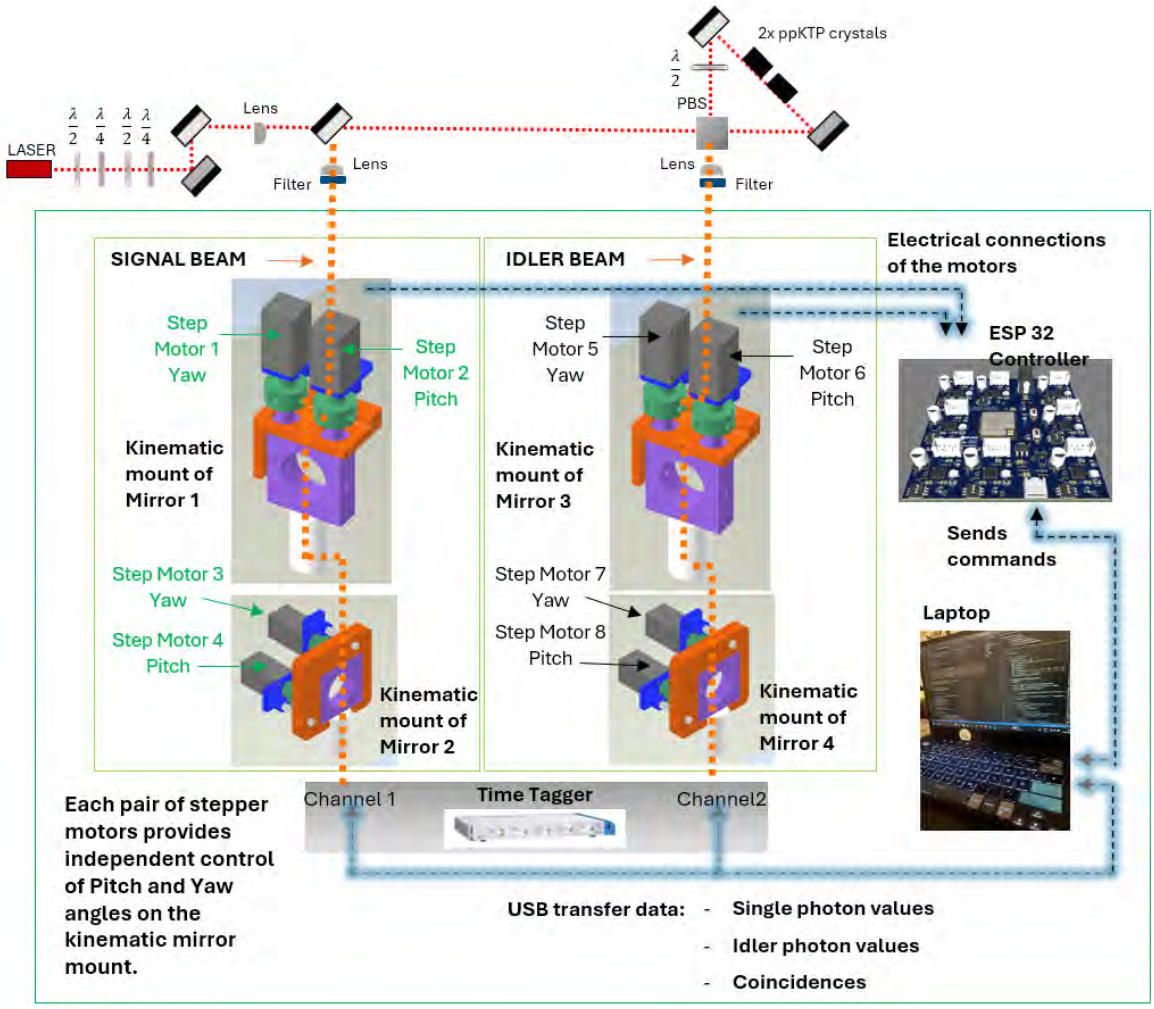

Figure 3.27: Assembled system of the system control for a quantum entanglement optical alignment system

Chapter 4

Verification and results

4.1 Theoretical Verification

4.1.1 Static Analysis of the 3D-Printed Mount

The results of the stress analysis were obtained assuming Tough PLA as the selected material. The properties considered in the simulation are as follows in the table 4.1.

Property	**Value**
Density	1.22 g/cm^3
Young's Modulus (E)	1.82×10^3 MPa
Poisson's Ratio	0.36
Yield Strength	37 MPa
Ultimate Tensile Strength	50 MPa

Tabla 4.1: Material Properties for Static Simulation analysis

The design dimensions of the 3D printed components were selected to minimize the use of workspace. During the experiments, breakages were observed due to improper human handling when the parts were placed on the kinematic mirrors. It is important to note that these initial prototypes were printed with only 50

The following images represent simulations of forces due to accidental human interaction, such as pressure or bending during assembly or maintenance, and the final version with 100

1. **External force for Main Support for Radiant Dyes Laser Kinematic Optical Mirror:**

   The following images illustrate the stress distribution under potential failure scenarios due to improper handling when placing the designed structure onto the optical mirror mount.

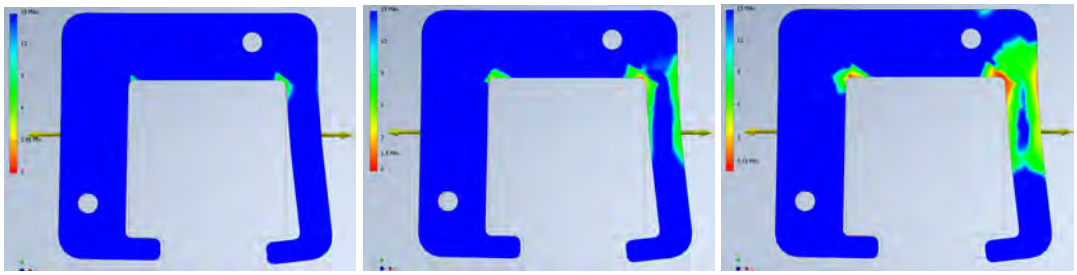

a. Corresponds to a 50N applied force with a minimum safety coefficient of 2.99

b. Corresponds to a 100N applied force with a minimum safety coefficient of 1.5

c. Corresponds to a 200N applied force with a minimum safety coefficient of 0.75

Figure 4.1: Structural Analysis of Main Support for Radiant Dyes Laser Kinematic Optical Mirror - safety factor

The analysis in figure 4.1 indicates that as the applied force increases, stress concentration becomes more pronounced, particularly in the thinnest regions of the part. The minimum safety factor is observed at the corner of the thinnest section, suggesting that this area is the most critical under excessive loading.

The analysis in figure 4.2 shows that the component is more prone to failure. However, this scenario would only arise due to improper handling, since the component is not intended to be subjected to such a force in that manner.

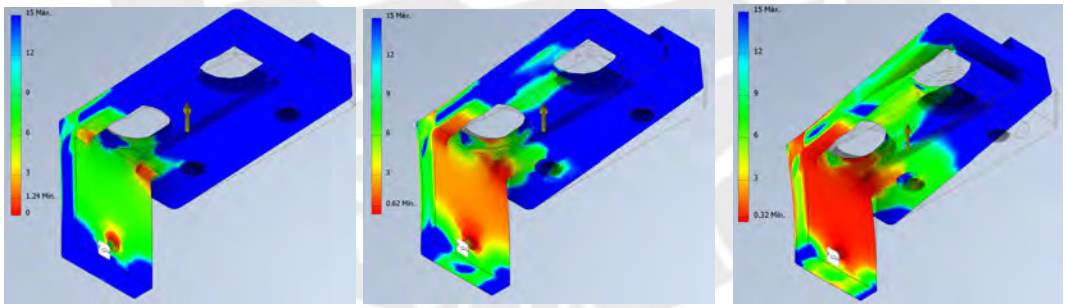

a. Corresponds to a 50N applied force with a minimum safety coefficient of 1.24

b. Corresponds to a 100N applied force with a minimum safety coefficient of 0.62

c. Corresponds to a 200N applied force with a minimum safety coefficient of 0.32

Figure 4.2: Structural Analysis of Main Support for Thor Labs Kinematic Optical Mirror

2. **Static analysis, normal conditions:**

The simulations corresponds to the 3D printed additional support, they are designed solely to support motors with a mass of approximately 60 grams. Therefore, the functional loads on this part are minimal (approximately 0.6 N) and do not represent a significant source of structural failure.

The Kinematic commercial optical mount on which the 3D printed parts are installed was not analyzed, as it was not modified, redesigned, or part of the study.

The simulations focus exclusively on evaluating the mechanical resistance of the printed parts to potential human errors during installation and assembly. The following images in figure 4.3 show the stress analysis of the other components; however, they are not affected by the weight of the motor.

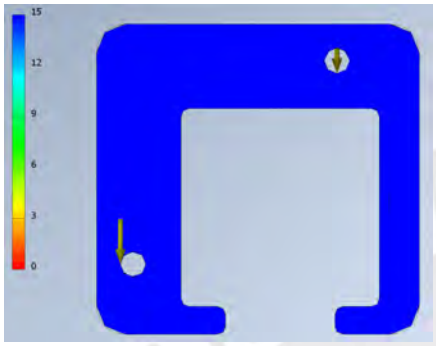

a. Static Analysis of Main Support 1

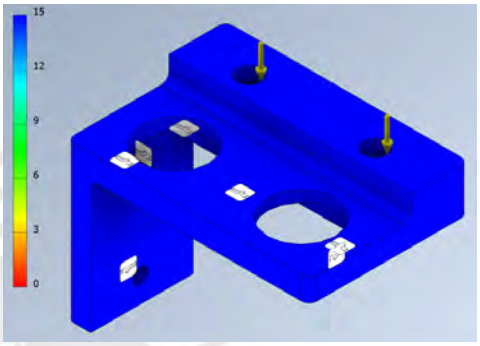

b. Static Analysis of Main Support 2

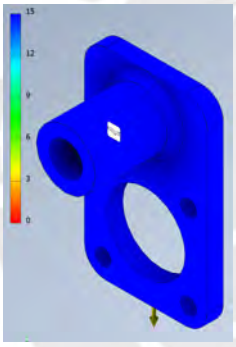

c. Static Analysis of Motor Coupling part

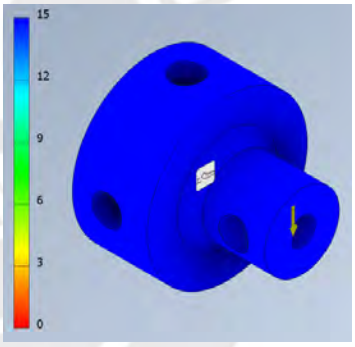

d. Static Analysis of Step Motor Support

Figure 4.3: Static Analysis of 3D printed parts - safety factor

4.1.2 Validation of Control Design

- **System Description:**
  - The control logic was designed to maximize the photon count values and the photon coincidences by iteratively aligning mirrors.
  - The behavior of the signal received from the detectors of the Qutag time tagger device, whether from channel 1 or channel 2, is modeled as a Gaussian curve.
  - Noise was added to the simulated signal, the Gaussian curve, to replicate real laboratory conditions, where the real system is very sensitive to ambient light.

- **Hypotheses and Assumptions:**
  - The peak of the Gaussian signal was assumed to represent the best possible alignment.
  - The motors respond to control commands based on trend analysis, using a filter to reduce noise before making decisions.
- **Expected Simulation Results:**
  - The control system should control the rotation of the motors until it finds the range where the peak value of the Gaussian simulated signal occurs. This range represents the maximum photon count, which also means a proper mirror alignment.
  - The system should be able to identify increasing or decreasing trends based on filtered data.

4.1.3 Logic of Alignment Control

The first part of the logic aligns each motor individually to achieve the peak of the Gaussian curve. Once the reference is obtained, the motors are aligned sequentially in both channels, alternating between them to visualize the changes in photon counts and coincidences.

1. **Initial Setup - Initial user interface:**

   These user-defined parameters are critical for ensuring the system's safe operation and accurate alignment during the simulation and control process. Through the interface, users define:

   - The USB connection settings for the Python code to communicate with the ESP32 device via USB, ensuring proper data transmission and motor control.
   - The initial direction of the motor's movement to prevent the knob attached to the motor from reaching its mechanical limits, protecting the hardware from excessive strain. This criterion is used to evaluate whether the current photon count value is greater or less compared to the initial value. In this way, the system will detect if the photon counts values are increasing or decreasing. The user inputs true or false depending on whether the motor starts moving to the right or to the left.
   - The first threshold is reached when the current value hits the limit. At this point, the final trend is evaluated to determine whether to continue in the same direction or change it if the trend is decreasing.
   - The threshold (peak_threshold) between the peak value and the current value, which determines when the motor should change direction and move toward the peak.

- The resolution, which specifies the range near the data or the motor's step count to decide when the motor is considered aligned.

The user interface, shown in Figure 4.4, plays a crucial role in configuring the initial parameters and connections of the system to align each motor first. The com port number, thresholds and desired resolutions are manually entered into the system.

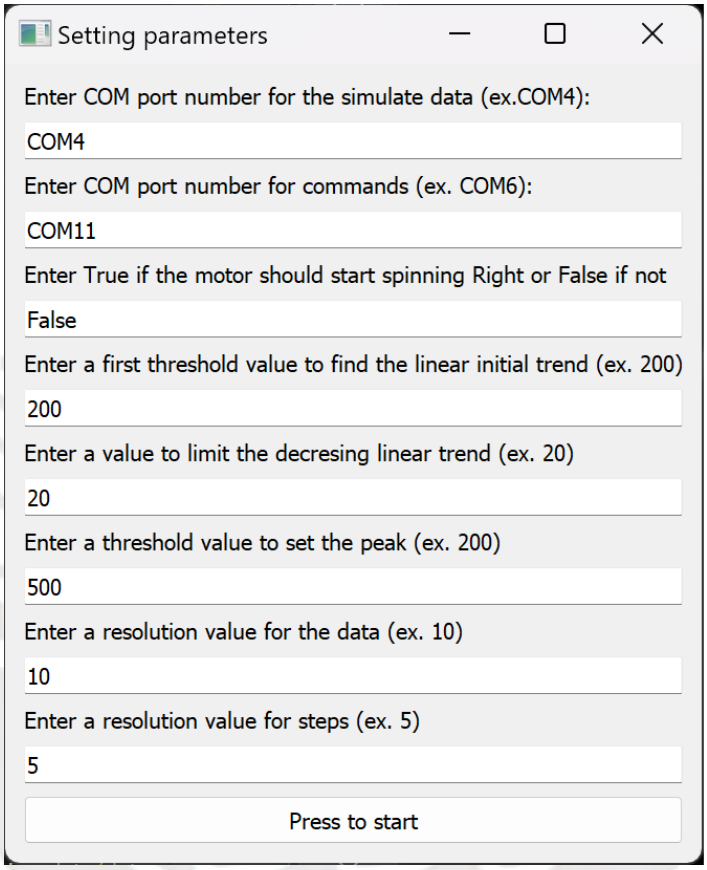

Figure 4.4: The user interface where you configure the parameters

2. **System flags:**

To ensure that the system responds correctly to alignment detection and avoids communication failures or data noise, several control flags are used. These variables help define the current state of the motor, evaluate trends, and decide when to stop. The following table 4.2 describes the most relevant system flags.

Variables/ Flags	Function
firstdata	A flag is used to determine if this is the first iteration. It is deactivated after reading the first data given by the time tagger device.
initrendflag	It is deactivated once the initial trend has been identified, whether it is increasing or decreasing.
ListWindowPair	It is a list where the current value read from the time tagger and its corresponding motor step count are grouped in pairs. a list of approximately 20 pairs.
majoritytrend	Determine whether the current trend is increasing or decreasing based on five previous criteria.
ListMayorTrend	List that stores previous trends, allowing for the evaluation of growth or decline patterns.
turn_to	The variable follow the logic to change its value when a change in direction is required. If the trend in ListMayorTrend is decreasing, the motor immediately reverses direction.
alldecrease	This flag counts the numbers of decreasing trends and when reach the limit, the process will stop.
peak_total	It is the previously found peak value.
peakfoundflag	The flag is triggered when the difference between peak_total and the current data is greater than a peak_threshold threshold.
Stopflag	The flag stop the motor.

Tabla 4.2: System flags

3. **Evaluating Current Values Against the Peak:** As the motor rotates, the current value is continuously compared to the highest recorded peak value. If the current value exceeds the peak, the motor continues rotating in the same direction.

4. **Threshold-Based Stopping:**

   - If the current value decreases and the difference from the previous peak is within a secondary threshold (indicating that the motor is moving away from the peak), the motor changes direction and moves back toward the peak.
   - The motor stops when it is near the highest recorded peak value, either by position (steps) or proximity within the desired resolution.

5. **Final State:**

   - Once the motor stops near the peak, the position is saved and the next motor is aligned. The first 4 motors are connected to the signal and the other 4 are connected to the idler.

The following image shows the flow chart of the logic to obtain the highest value of photons using a motor. This logic will be repeated in the 8 motors to obtain the desired values representing the alignment of the optical mirrors.

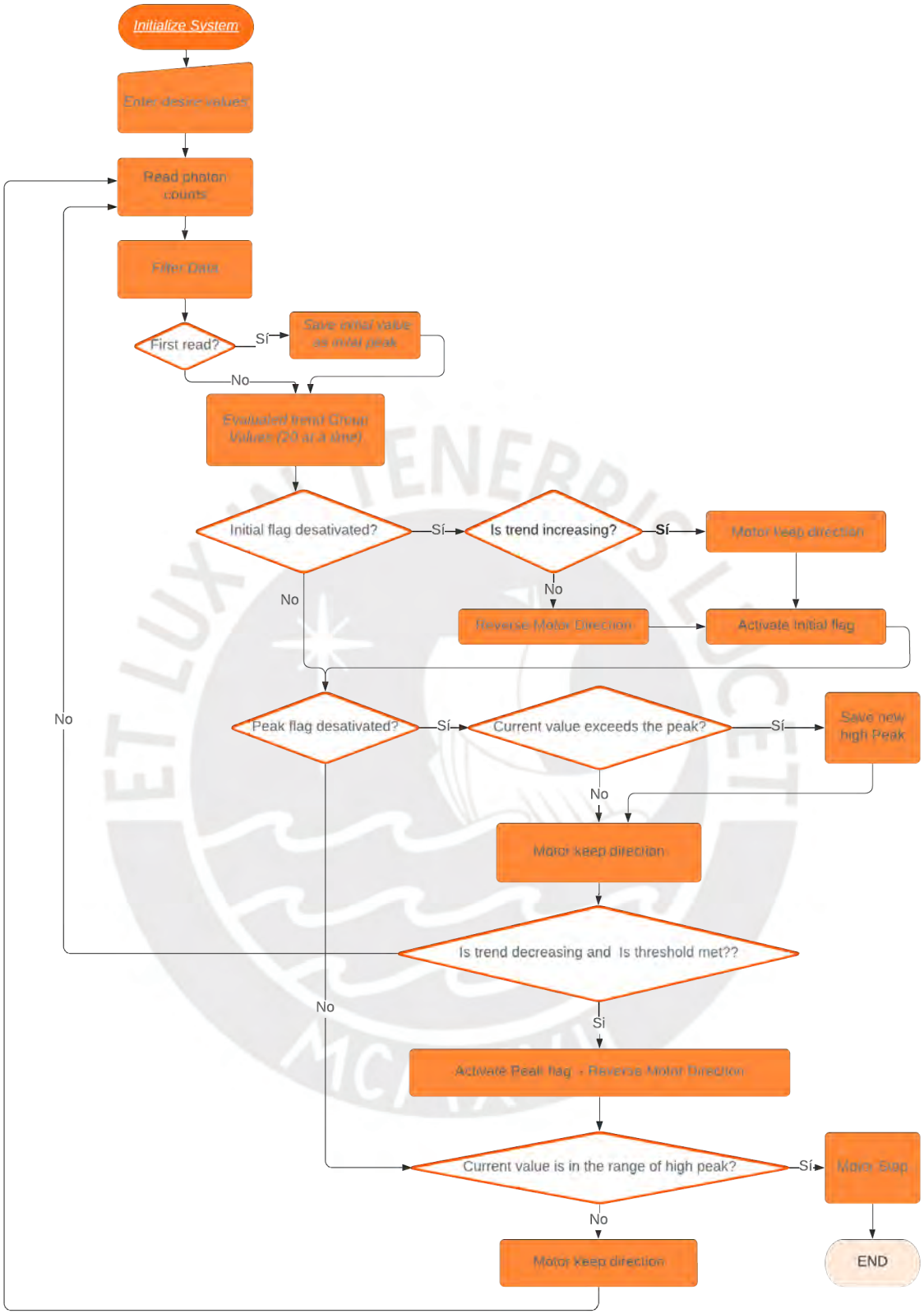

Figure 4.5: Alignment control flow chart

4.2 Simulation-Based Verification

4.2.1 Signal Processing and Filtering

- **Data Acquisition Process**

  Initially, the mirrors were manually aligned as accurately as possible to ensure that a peak would be detected when the motor completed its full motion. Then, the optical mirror mount knobs were rotated manually to one side. Using the first part of the logic code, the motors were commanded to rotate to the opposite extreme, while recording the data from the Time Tagger Qutag. The data for each motor were stored separately, and the Gaussian shape of the data was verified for each.

- **Data Filtering and Processing**

  Since the data exhibited large variations, a median filter was first applied to reduce noise. However, due to the high range of variation in the data, a second filter, Savitzky-Golay, was applied to further smooth the signal while preserving its characteristics. Finally, a Gaussian fit was performed to establish a reference point for alignment.

- **Procedure for Each New Configuration**

  These experiments must be conducted each time a new mirror mount position is set. The data is collected in real-time, one point at a time, every 100 ms. After acquisition, the data is filtered, analyzed to determine the trend, and the peak value is stored. This peak value serves as a reference for the alignment of each motor controlling the mirrors.

4.2.2 Motor Alignment Simulation

In some experiments, the photon count peak reached values around 7000, while for other experiments, it was approximately 2500. This difference may be attributed to variations in optical alignment, detector sensitivity, or signal intensity. These discrepancies were carefully analyzed to ensure accurate photon detection and system optimization.

The following graphs in the figure 4.6 show the value of the data obtained according to the motor movements, whether it starts rotate clockwise or counterclockwise. The process continuously stores the highest photon counts values and will command to keep the same direction of the rotation of the motor, until the trend analysis remains decreasing and the current photon count value drops below the last recorded maximum (beyond a certain margin).
In the upper graphs (a) and (b) of the figure 4.6, the photon count values of the Gaussian curve readings are plotted.

In the lower graphs (c) and (d) of the figure 4.6, the motor position index is plotted as a linear progression that reflects the direction of rotation. This index is a numerical value initialized in 70000 by programming, used to simulate the motor step count. The value increases steadily while moving in one direction and decreases when the motor is reversed.

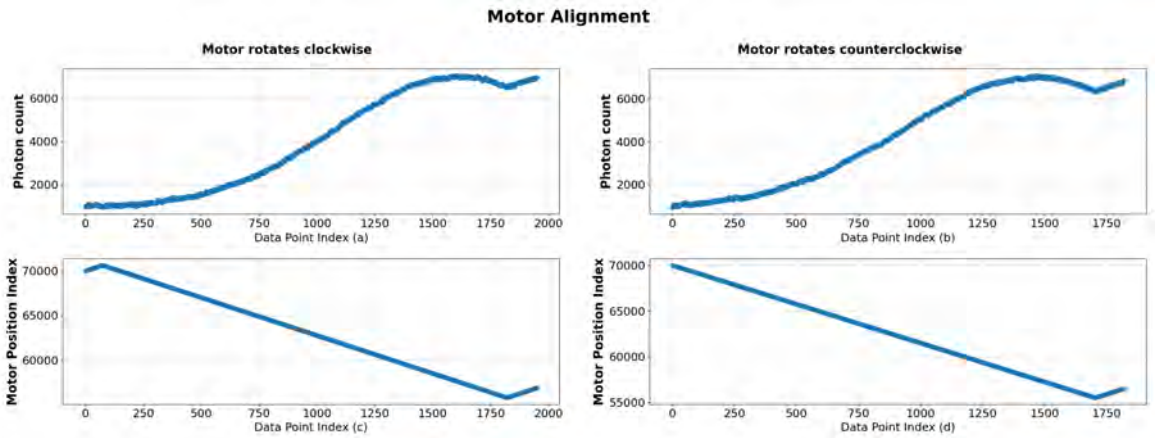

Figure 4.6: Photon Count and Step Data Based on Motor Movements

4.2.3 Simulation Results Summary

In this section, a screenshot of the user interface is presented in Figure 4.7, showing the values found during the simulation. The interface shows the relevant parameters and results, providing a clear view of the performance of the system and the detected peak values.

- The motor with which the experiment is working is specified to verify that it is working correctly.
- In addition, the initial trend of the data is specified, that is, whether they increase or decrease. If the data begin to decrease, a message is sent indicating that the motor has changed direction.
- Also, as the values are saved automatically, the value of the counter is shown where significant changes occur such as the change in rotation of the motor, in this way to be able to review the behavior if necessary.
- The logic of the system seeks to identify the maximum photon count value and stop the motor only when it detects a continuous downward trend. Once the motor stops, a comparison will be displayed between the value at which it stopped and the maximum value recorded previously. This allows us to verify that the system did indeed identify and return to the position corresponding to the maximum photon count.

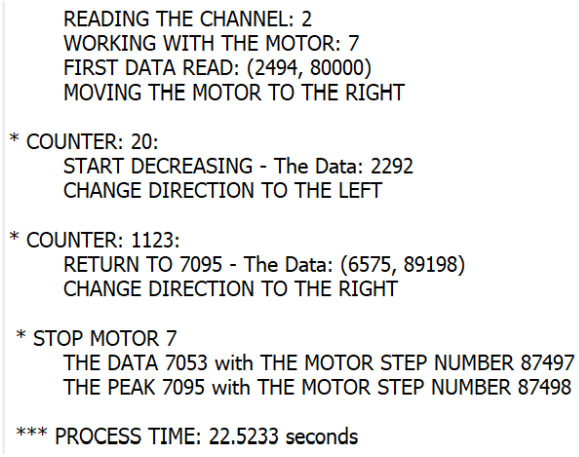

Figure 4.7: User interface with results

4.2.4 System Alignment Simulation

In the second part of the process, once the reference is obtained from the first part, the motors are moved alternately between channels. However, the system always targets the highest value detected and compares it with the reference value to check for possible improvements. If a higher value is found, the system updates the reference; otherwise, it maintains the original range reference.

In the upper section of the image, the yellow graph shows the values of the coincidences. The data is increasing and decreasing according to the alignment of the mirror when a motor moves, considering that when the mirrors are aligned, the maximum value of matches will be obtained.

The following graphs show the photon count of the signal detected on channel 1 and idler detected on channel 2.

The alignment process is performed in sequence and starts with moving motor 1 of mirror 1, which affects the signal detected on channel 1, followed by motor 1 of mirror 3, idler detected by channel 2, and so on.

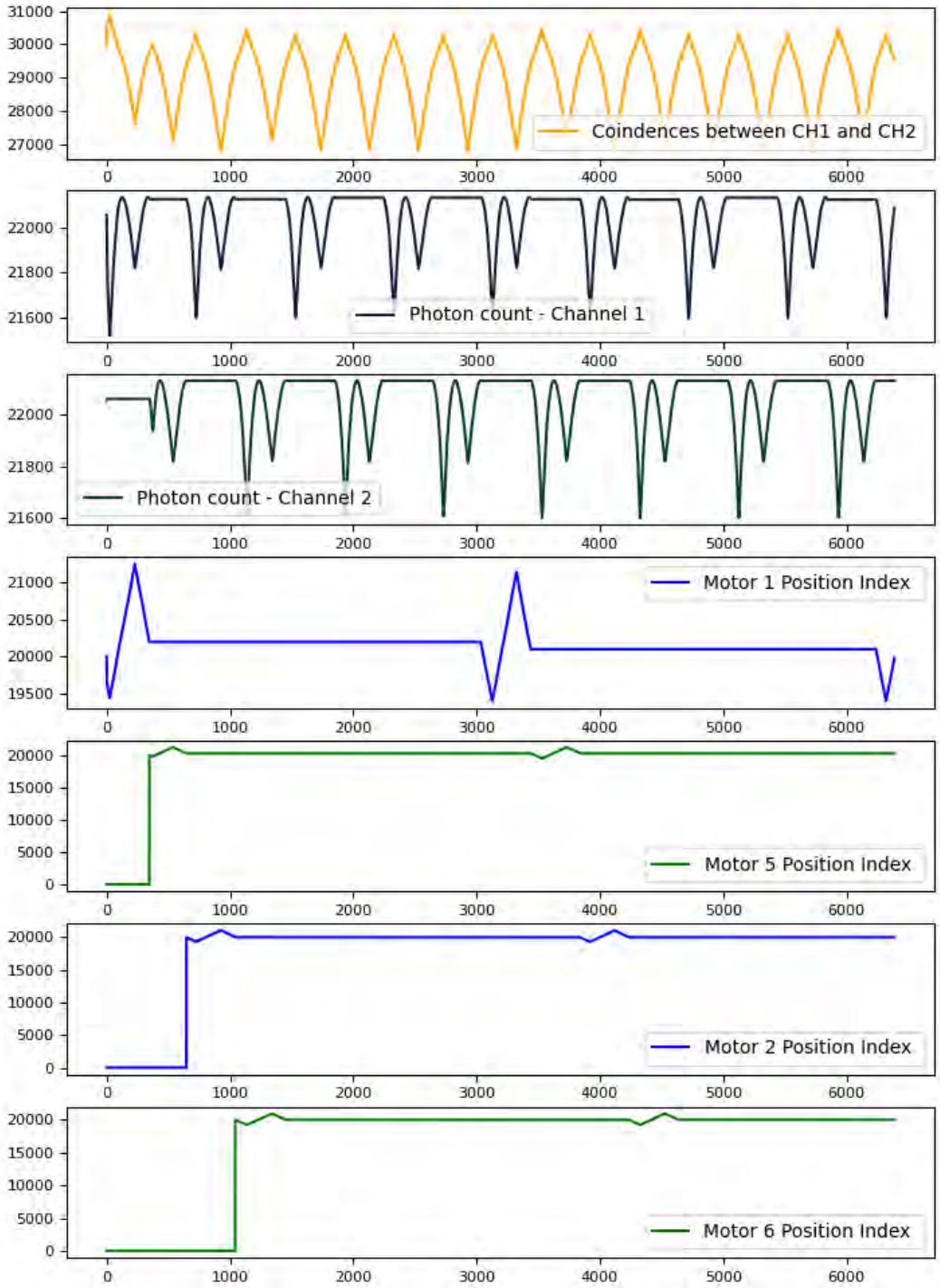

Figure 4.8: Alignment Results of Coincidences and Photon counts with their respective motors movements

4.3 Analysis of Results

4.3.1 Analysis of Results with optimal Parameters

Presents simulation results of the movement of the motors with different initial rotation:

1. **Initial step motor movement and trend assessment:**

   A zoomed-in view of Figure 4.6 highlights the initial part of the process. At this stage, the system evaluates whether the initial trend is increasing or decreasing by analyzing the grouped data. This analysis is crucial for determining the motor's starting direction. The intersection or break in the line occurs when the motor changes direction upon detecting that the signal trend is no longer increasing.

   In Figure 4.9, part (a) shows the data when the motor rotates clockwise. The detection of a decreasing trend prompts a change in the motor's direction as shown in part (b), t is highlighted in the green box. On the other hand, when the same motor starts rotating counterclockwise, the system detects an increasing trend in the data, as shown in part (c). Consequently, there is no change in the motor's direction, as illustrated in part (d).

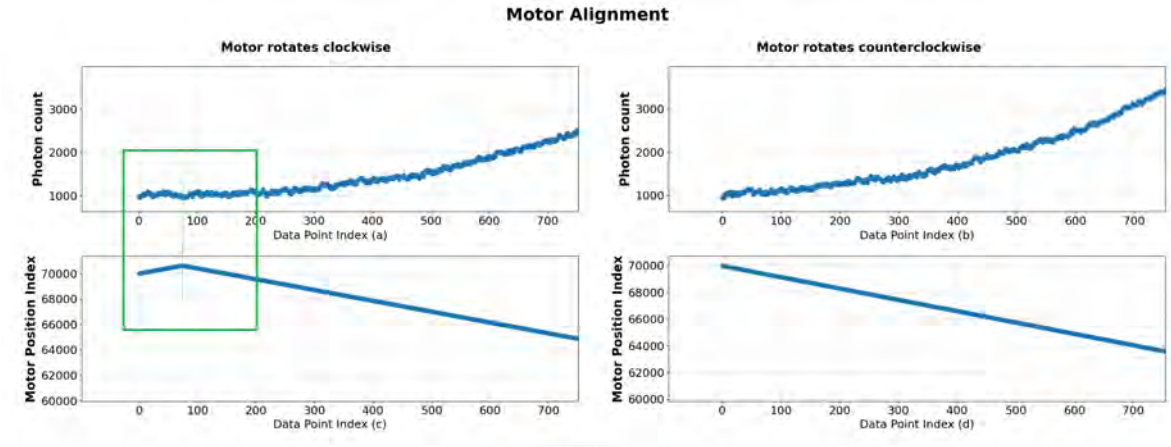

Figure 4.9: Initial step motor movement and trend assessment

2. **Peak detection and direction reversal:**

   Similarly, a zoomed-in view of the final part of the Figure 4.6 reveals that the motor continues rotating in the same direction as long as the trend remains increasing. The motor only changes direction when the trend decreases, and the user-defined threshold between the current value and the detected peak is reached. At this point, the motor returns to the previously detected peak value or within the specified range defined by the user at the beginning.

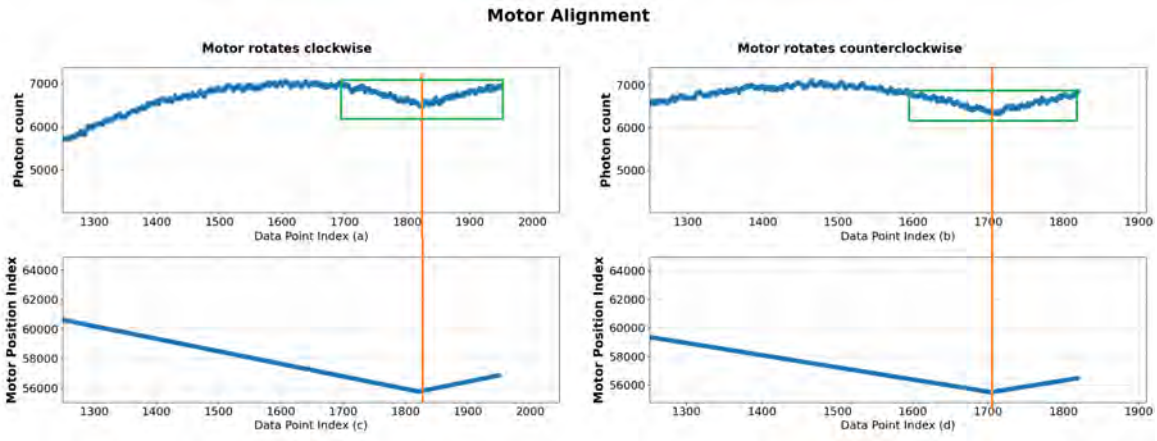

Figure 4.10: Final step motor movement and trend assessment

In Figure 4.10, an orange line indicates when the current value reaches the limit defined by the user, meaning that the current value minus the peak value equals the threshold.

Additionally, the green boxes highlight when the motor stops after detecting a value within the range defined by the user, whether it is the value itself or its position.

4.3.2 Analysis of Results with Varying Parameters

Additional analysis have been included to illustrate the system's behavior under different initial parameter configurations in the user interface. These visualizations compare how changes in parameters influence the final results. This analysis provides insights into the system's robustness and helps identify the optimal settings for improved performance.

1. **Varying parameters 1:**

   The following parameters from the user interface have been updated and are shown in Table 4.3.

	Parameters 1	**Parameters 2**
First Threshold to identify the intial trend	200	100
Threshold to set the peak	500	800
Data resolution	10	20
Steps resolution	5	10

Tabla 4.3: Comparative analysis using different parameters

The figure 4.11 shows the output user interface that displays the results of channel 2 using motor 7 using the parameters in the table 4.3

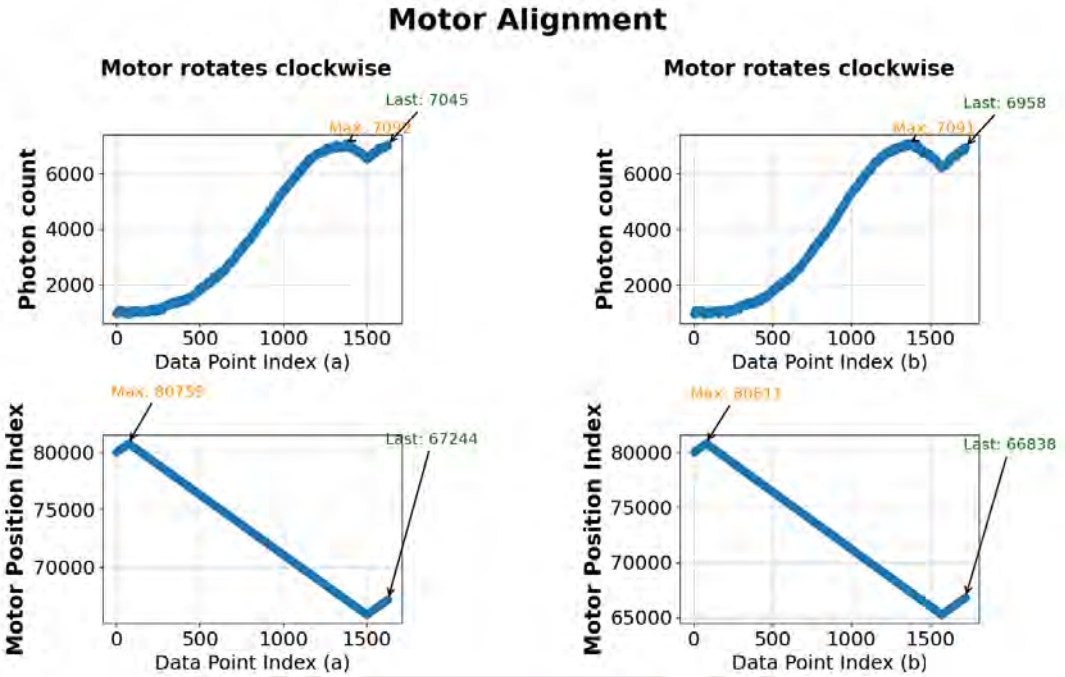

Figure 4.11: Comparative analysis - graphic results with good parameters

In figure 4.11 shows the results where the second configuration reaches the target peak faster but with a slightly lower peak value. Despite this, the final peak value found in both cases falls within the acceptable range defined by the user. This observation is significant for optimizing the independent alignment of each motor before moving on to align all motors consecutively. Proper selection of these parameters can enhance the likelihood of achieving a higher number of coincidences when all motors are aligned sequentially.

2. **Varying parameters 2:**

   For channel 1 using motor 2, if the threshold and the data resolution are too large, the system may miss the peak and fail to reverse the motor's direction. As a result, the code will stop running after a user-defined number of consecutive decreasing trend counts. In Figure 4.12, the results of the graphical curve can be observed.

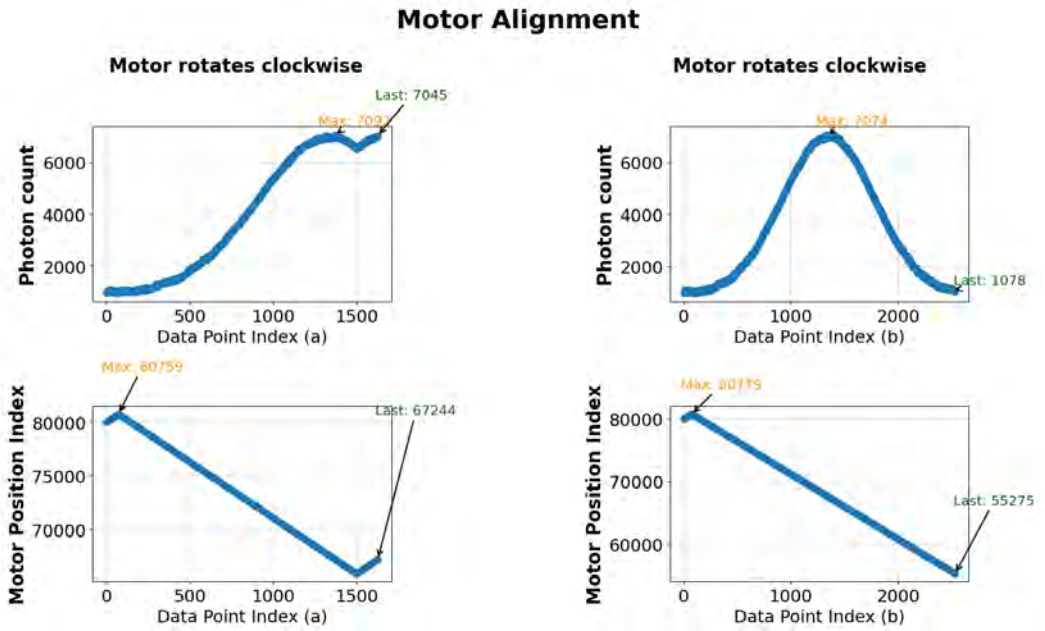

Figure 4.12: Comparative analysis - graphic results with bad parameters

The results are shown in Figure 4.13, which displays the user interface with detailed information.

```
* SAVING DATA IN THE NEXT FOLDER:
      C:\Users\monta\OneDrive\Escritorio\ESCRITORIO\ALIGN
MANUAL\DISCQOASys_SIM\SIM_TF_DATA\G12
* CREATE THE FILE: data_G12_test_1.txt
* It has a max of 4 files backups

      READING THE CHANNEL: 1
      WORKING WITH THE MOTOR: 2
      FIRST DATA READ: (941, 70000)
      MOVING THE MOTOR TO THE LEFT

* COUNTER: 80:
      START DECREASING - The Data: 922
      CHANGE DIRECTION TO THE RIGHT

* COUNTER: 1525:
      RETURN TO 6865 - The Data: (6552, 55878)
      CHANGE DIRECTION TO THE LEFT

* STOP MOTOR 2
      THE DATA 6858 with THE MOTOR STEP NUMBER 56614
      THE PEAK 6865 with THE MOTOR STEP NUMBER 58645

*** PROCESS TIME: 33.1029 seconds
```

a. Output results 1

```
* SAVING DATA IN THE NEXT FOLDER:
      C:\Users\monta\OneDrive\Escritorio\ESCRITORIO\ALIGN
MANUAL\DISCQOASys_SIM\SIM_TF_DATA\G12
* CREATE THE FILE: data_G12_test_4.txt
* It has a max of 4 files backups

      READING THE CHANNEL: 1
      WORKING WITH THE MOTOR: 2
      FIRST DATA READ: (941, 70000)
      MOVING THE MOTOR TO THE LEFT

* COUNTER: 87:
      START DECREASING - The Data: 1014
      CHANGE DIRECTION TO THE RIGHT

- BREAK through the 1000 decreasing trends
```

b. Output results 2

Figure 4.13: Comparative analysis - user interface with results

4.3.3 Analysis of Results of the second part of the logic alignment

A zoomed-in figure 4.14 and 4.15 of the graph highlights key observations: when the photon value decreases, the motor moves back to the previously detected peak point. The flat regions in the photon data indicate moments when no motor in the current channel is moving, maintaining stability at the peak value. Notably, changes in photon counts occur only when the corresponding motor moves, demonstrating the independence between channels.

1. **Channel 1 Data:**

   This graph illustrates the photon counting data for channel 1 alongside the movements of the four respective motors (index 1 to 4).

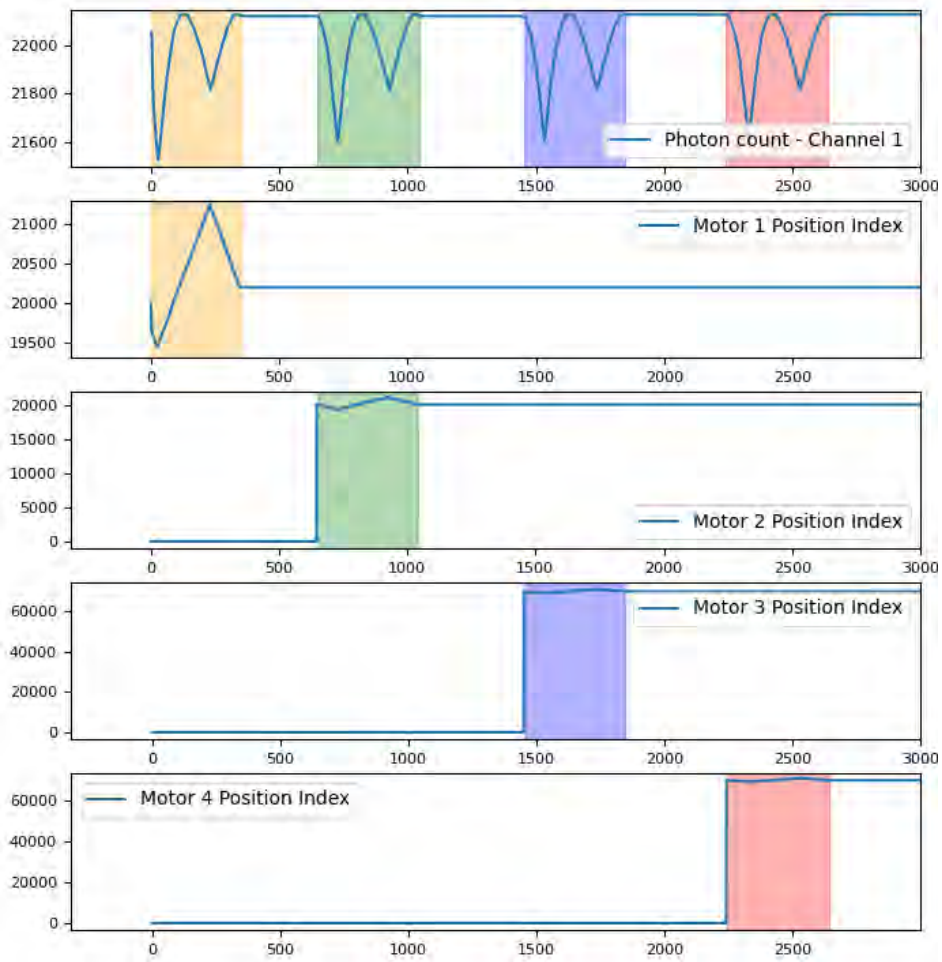

Figure 4.14: Regions that specify the change of data in channel 1 according to the movement of its motor responses

2. **Channel 2 Data:**

   This graph presents the photon counting data for channel 2 along with the motor movements specific to this channel (index 5 to 8).

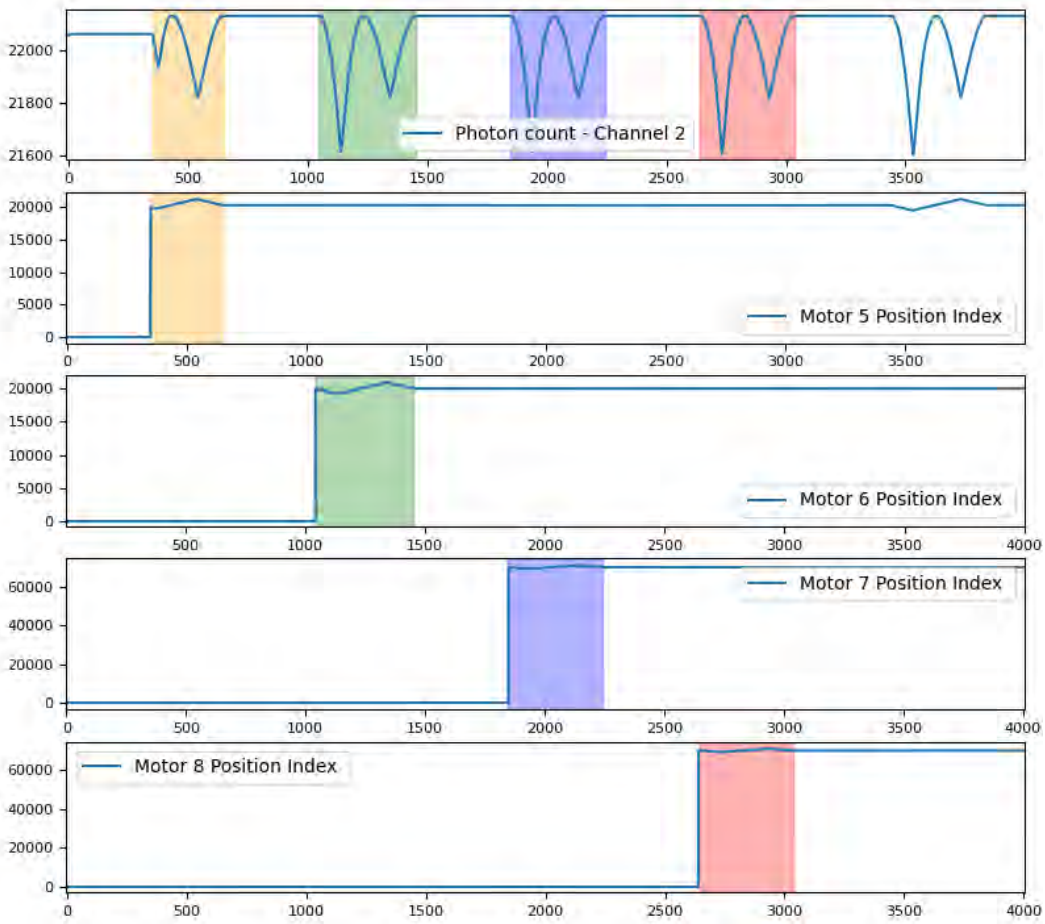

Figure 4.15: Regions that specify the change of data in channel 2 according to the movement of its motor responses

4.3.4 Limitations and potential improvements

When carrying out the study with the different technical parameters, limitations are observed in the simulation as in the real world, in this way possible future work is presented, which is detailed below.

1. **Limitations of the Simulated Approach**

   One limitation of the current simulation is that it uses the same dataset for each test, leading to consistent peak detection and similar curve behavior. Although this helps to assess the performance of the system under controlled conditions, it may not fully capture the variability that would be present in real-world scenarios.

   However, simulations have inherent limitations. The synthetic data simplifies noise characteristics, leading to more predictable results that may not fully capture the complexity

of real-world noise. Additionally, the simulation relies on manually adjusted parameters (such as thresholds and resolution), which might not be optimal in diverse scenarios.

2. **Real-World Limitation**

   It is observed that the photon count varies despite there being no movement in the mirrors. This means that when the motor is moving in search of a maximum value, a peak can be recorded at a certain point. However, when the motor returns to that same position to confirm the maximum value, the reading may have changed even though it is at the same physical point.

   To mitigate this effect, a tolerance range is defined both in the measured values and in the position of the motor, the problem of defining these ranges is only obtained through several tests and data analysis. This allows establishing more robust criteria to identify the optimal value, ensuring that the alignment process is more stable and less susceptible to fluctuations in the signal.

3. **Potential Improvements**

   - Testing the system in a laboratory setting with real-world data is essential. Evaluations should account for environmental factors not fully captured in the simulation, such as sensor noise, temperature fluctuations, and mechanical tolerances. By obtaining a larger number of samples of real data, the robustness of the algorithm could be improved and evaluated in more complex conditions.
   - Currently, microstepping is fixed manually; To control it digitally, more output pins are required. This implies the need for a microcontroller with more pins or the use of an additional microcontroller. In this way, the control of the motors could be divided.

     In the current configuration, the fixed microstepping determines the speed of the motor, keeping it constant. To modify the speed, it would be necessary to change the microstepping automatically by code. This, in turn, requires a different control architecture.

Chapter 5

Conclusions and recommendations

5.1 Conclusions

From the work presented, the following conclusions are obtained.

- **System Validation** The system successfully aligns the signal and idler photons by maximizing their coincidence counts. The logic behind the code ensures that the alignment improves by prioritizing higher coincidence values. As the system acquires data, it continuously compares new values with previous ones, following a decision-making process that determines whether the alignment is improving. If the coincidence count increases, the system confirms that the alignment is moving in the correct direction. Otherwise, it adjusts accordingly.

- **Algorithm Performance** The time tagger detects and processes photon events, generating a Gaussian-like curve as the mirror moves across its range. Since the raw data fluctuates significantly, a filtering process is applied to smooth the data. The algorithm tracks increasing trends and continuously stores and compares incoming data in real-time. Maximum values are recorded along with the position of the stepper motor, allowing a precise identification of the alignment peak.

- **Automation and Optimization** Once the system detects the maximum coincidence values, the stepper motor returns to the optimal position recorded. This is based on prior analysis and real-time comparisons, ensuring that the best alignment is restored. The total processing time ranges from approximately 20 to 50 seconds, depending on the initial manual alignment of the mirror. Although manual pre-alignment is not perfect, it helps ensure that the system will eventually locate the coincidence peaks.

- **Movement Correction** The system is capable of dynamically correcting its movement if it detects a decrease in coincidence counts. By analyzing data patterns and detecting increasing or decreasing trends, it can adjust the mirror's position accordingly. Experimental results include images that demonstrate the detection of alignment peaks and the system's ability to return and correct its position based on observed trends. Additionally, if the coincidence count decreases beyond a user-defined threshold set in the interface, the motor will automatically stop. This feature was simulated to ensure that the system can handle potential failures, such as incorrect values from the microcontroller or unstable connections. The simulation confirmed that, under these conditions, the system successfully stops operation to prevent misalignment or hardware issues.

- **Design Feasibility** The mechanical design utilizes 3D-printed components, making it highly adaptable to different optical mirrors with two-axis movement. Additionally, the electronic design was developed using components that are readily available in the market, ensuring practical feasibility. The initial Version 1 of the system follows this modular approach, while Version 2 integrates all components into a compact, single-unit design, making it even easier to manufacture and assemble.

- **Motor accuracy and speed** Although there are industrialized options of high precision and speed, such as piezoelectric motors or DC motors, in this work it has been shown that the use of stepper motors together with their controllers allows a resolution of less than 1 arcsecond to be achieved.

  In this case, the accuracy in the final position is the key factor and not the speed of the motor. Unlike a DC motor, where advanced control strategies need to be implemented to regulate speed and stop accurately, a stepper motor allows you to move directly to a specific position without the need for a complex feedback system. Thanks to this, the total time of the alignment process has been significantly reduced.

5.2 Recommendations

Since this work has been mainly based on simulations considering the real limitations and has been partially experimented (since the printing and testing were carried out in the system, but multiple samples and optimal results could not be obtained due to lack of testing), the following recommendations are presented based on the observations during the process.

1. **Electrical connections and short circuit prevention:**

    - It is crucial to visually check that all cables are properly connected and that there are no signs of wear or damage to the cables' insulation. In addition, connections should be checked for loose spots, as this could cause unstable connections or short circuits.
    - It is recommended to use high-quality connectors and to secure all cables well to prevent movements that could cause short circuits.
    - To ensure the integrity of the electronic board, it is ideal to have an overload or short circuit protection system, if possible, to prevent damage in the event of a fault.

2. **Manual alignment of mirrors and significant photons:**

    - Before starting the alignment with the automated code, it is recommended to perform a fine manual alignment to ensure that the mirrors are correctly positioned. This can be done using a photon meter to ensure that a significant amount of photons are being detected, which is essential for accurate results.
    - Make sure that the mirrors are aligned in a way that maximizes the photon signal and minimizes possible noise values. If the mirror is not aligned correctly, the system could detect a higher level of noise, which would affect the measurements.

3. **Using Python code for individual motor alignment:**

    - It is recommended to start by aligning motor by motor using specific Python code that records reference values for each motor. This helps to get accurate initial positions before using the general code, which compares photon matches acr oss the system. This will allow you to fine-tune each motor before running the full process.

4. **Additional Recommendations:**

    - **Temperature Monitoring:** Make sure to monitor the temperature of your system and electronic components, as overheating could affect their performance or even damage them.

- **Periodic Calibration Testing:** Perform calibration tests on your system over time, especially if you notice that the results are starting to deviate from expectations. This will ensure that your system remains properly aligned as the process progresses.
- **Data Backup:** Keep a backup of key data and settings before making major changes to your system, in case you need to restore them later.

[30] [31] [32] [33] [34]

Bibliography

[1] A. Einstein, B. Podolsky, and N. Rosen, "Can quantum-mechanical description of physical reality be considered complete?," *Physical Review*, vol. 47, no. 10, pp. 777–780, 1935.

[2] W. Tittel and G. Weihs, "Photonic Entanglement for Fundamental Tests and Quantum Communication," Tech. Rep. 0, 2001.

[3] R. Fickler, M. Krenn, R. Lapkiewicz, S. Ramelow, and A. Zeilinger, "Real-time imaging of quantum entanglement," *Scientific Reports*, vol. 3, 2013.

[4] T. L. Parnell, B. J. Smith, and I. R. Petersen, "Entangled photon apparatus for the undergraduate laboratory," *Am. J. Phys.*, vol. 70, pp. 898–902, 2002.

[5] Z.-Y. Zhou, Y. Xia, Y.-Q. Li, W. Wang, X. Ma, B.-H. Liu, T. Xu, Y.-S. Zhang, and J.-W. Pan, "Experimental feasibility of molecular two-photon absorption with isolated time-frequency-entangled photon pairs," *Phys. Rev. A*, vol. 77, p. 033845, Mar 2008.

[6] D. Chin, "Optical mirror-mount design and philosophy," *Optics and Photonics News*, vol. 4, no. 11, pp. 34–38, 1993.

[7] L.-W. Wei, K. Karan, and B. Willke, "Optics mounting and alignment for the central optical bench of the dual cavity enhanced light-shining-through-a-wall experiment alps ii," *Review of Scientific Instruments*, vol. 87, no. 9, p. 095116, 2016.

[8] F. A. DeWitt, "A novel mirror-mount design suitable for laboratory and oem applications," *Review of Scientific Instruments*, vol. 78, no. 3, p. 033105, 2007.

[9] G. C. Anzalone, A. G. Glover, and J. M. Pearce, "Open-source colorimeter," *Sensors*, vol. 13, no. 5, pp. 5338–5346, 2013.

[10] A. K. Ekert, "Quantum cryptography based on bell's theorem," *Phys. Rev. Lett.*, vol. 67, pp. 661–663, Aug 1991.

[11] D. S. Naik, C. G. Peterson, A. G. White, A. J. Berglund, and P. G. Kwiat, "Entangled state quantum cryptography: Eavesdropping on the ekert protocol," *Physical Review Letters*, vol. 84, p. 4733–4736, May 2000.

[12] W. Tittel, J. Brendel, H. Zbinden, and N. Gisin, "Quantum cryptography using entangled photons in energy-time bell states," *Phys. Rev. Lett.*, vol. 84, pp. 4737–4740, May 2000.

[13] C. H. Bennett and S. J. Wiesner, "Communication via one and two particle operators on einstein-podolsky-rosen states," *Physical Review Letters*, vol. 69, no. 20, pp. 2881–2884, 1992.

[14] A. S. Holevo, "Bounds for the quantity of information transmitted by a quantum communication channel," *Problemy Peredachi Informatsii*, vol. 9, no. 2, pp. 31–42, 1973.

[15] C. H. Bennett, G. Brassard, C. Crépeau, R. Jozsa, A. Peres, and W. K. Wootters, "Teleporting an unknown quantum state via dual classical and einstein-podolsky-rosen channels," *Phys. Rev. Lett.*, vol. 70, pp. 1895–1899, Mar 1993.

[16] R. Horodecki, P. Horodecki, M. Horodecki, and K. Horodecki, "Quantum entanglement," *Rev. Mod. Phys.*, vol. 81, pp. 865–942, Jun 2009.

[17] V. Protopopov, *Beam Alignment and Positioning Techniques*, pp. 309–334. Cham: Springer International Publishing, 2014.

[18] J. Smith and A. Johnson, "Quantum mechanics with patterns of light: Progress in high dimensional and multidimensional entanglement with structured light," *AIP Advances*, vol. 1, no. 1, p. 011701, 2021.

[19] K. T. Bullock, R. J. DeYoung, and S. P. Sandford, "Angular alignment testing of laser mirror mounts under temperature cycling," Technical Publication 19970020045, NASA Langley Research Center, Hampton, VA, United States, June 1997.

[20] M. Gopalakrishnan and M. Gühr, "A low-cost mirror mount control system for optics setups," tech. rep.

[21] R. S. Mathew, R. O'Donnell, D. Pizzey, and I. G. Hughes, "The Raspberry Pi auto-aligner: Machine learning for automated alignment of laser beams," *Review of Scientific Instruments*, vol. 92, 1 2021.

[22] I. Galaktionov, V. Toporovsky, A. Nikitin, A. Rukosuev, A. Alexandrov, J. Sheldakova, A. Laskin, and A. Kudryashov, "Software and hardware implementation of the algorithm for 2-mirrors automatic laser beam alignment system," in *Proceedings of SPIE: Laser Beam Shaping XXIII*, vol. 12667, p. 126670I, 2023.

[23] C. Zhang, N. C. Anzalone, R. P. Faria, and J. M. Pearce, "Open-source 3d-printable optics equipment," *PLoS ONE*, vol. 8, no. 3, p. e59840, 2013.

[24] B. J. Winters and D. Shepler, "3d printable optomechanical cage system with enclosure," *HardwareX*, vol. 3, pp. 62–81, 2018.

[25] H. Y. Jeong, E. Lee, S.-C. An, Y. Lim, and Y. C. Jun, "3d and 4d printing for optics and metaphotonics," *Nanophotonics*, vol. 9, no. 5, pp. 1139–1160, 2020.

[26] H. Gao, J. An, C. K. Chua, D. Bourell, C.-N. Kuo, and D. T. Tan, "3d printed optics and photonics: Processes, materials and applications," *Materials Today*, vol. 69, pp. 107–123, 2024.

[27] D. A. Robb, D. Risbridger, B. Mills, I. Rakhmatulin, X. Kong, M. Erden, M. D. Esser, R. M. Carter, and M. J. Chantler, "Three approaches to the automation of laser system alignment and their resource implications: A case study," in *2024 IEEE 20th International Conference on Automation Science and Engineering (CASE)*, pp. 296–303, 2024.

[28] L. J. Salazar-Serrano, G. Jiménez, and J. P. Torres, "How to automate a kinematic mount using a 3D printed arduino-based system," *Inventions*, vol. 3, 6 2018.

[29] Allegro Microsystems, *A4988 DMOS Microstepping Driver with Translator Datasheet*, 2007.

[30] S. Mozes, J. Oppenheim, and B. Reznik, "Deterministic dense coding with partially entangled states," *Phys. Rev. A*, vol. 71, p. 012311, Jan 2005.

[31] Y. Guo, B.-H. Liu, C.-F. Li, and G.-C. Guo, "Advances in quantum dense coding," *Advanced Quantum Technologies*, vol. 2, no. 5-6, p. 1900011, 2019.

[32] Z.-S. Yuan, X.-H. Bao, C.-Y. Lu, J. Zhang, C.-Z. Peng, and J.-W. Pan, "Entangled photons and quantum communication," *Physics Reports*, vol. 497, no. 1, pp. 1–40, 2010.

[33] T. Jennewein, C. Simon, G. Weihs, H. Weinfurter, and A. Zeilinger, "Quantum cryptography with entangled photons," *Phys. Rev. Lett.*, vol. 84, pp. 4729–4732, May 2000.

[34] C. Schimpf, M. Reindl, D. Huber, B. Lehner, S. F. C. D. Silva, S. Manna, M. Vyvlecka, P. Walther, and A. Rastelli, "Quantum cryptography with highly entangled photons from semiconductor quantum dots," *Science Advances*, vol. 7, no. 16, p. eabe8905, 2021.